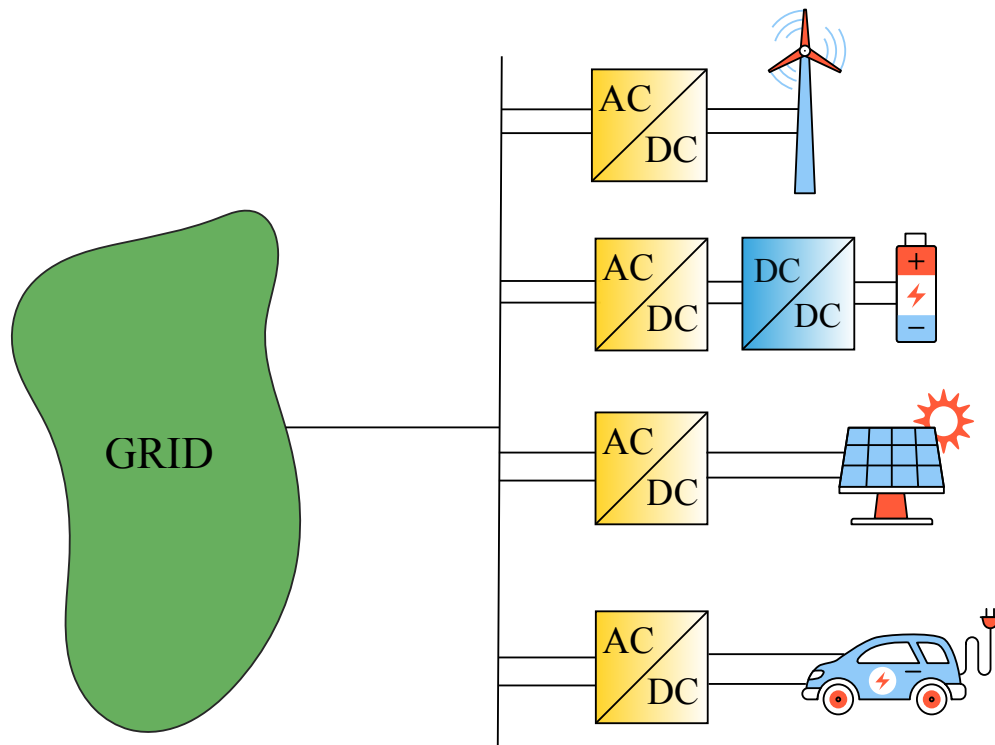




Universidad Tecnológica de Pereira
Programa de Ingeniería Eléctrica
Pereira, 17 July 2018



STABILITY ANALYSIS FOR SINGLE PHASE CONVERTERS IN MICROGRIDS APPLICATIONS

Master thesis presented as partial requirement for the title of Master in Electrical Engineering

By:
María Victoria Gasca

STABILITY ANALYSIS FOR SINGLE PHASE CONVERTERS IN MICROGRIDS APPLICATIONS

María Victoria Gasca

Thesis presented as a partial requirement
to qualify for the Master's Degree
in Electrical Engineering

Pereira, 17 July 2018
UNIVERSIDAD TECNOLÓGICA DE PEREIRA
Master's Program in Electrical Engineering.



STABILITY ANALYSIS FOR SINGLE PHASE CONVERTERS IN MICROGRIDS APPLICATIONS

©María Victoria Gasca

Supervisor: Alejandro Garcés Ruiz.

Co-supervisor: Marta Molinas.

Pereira, 17 July 2018

Programa de Ingeniería Eléctrica.

Universidad Tecnológica de Pereira

La Julita. Pereira(Colombia)

TEL: (+57)(6)3137122

www.utp.edu.co

Versión web disponible en: *<http://recursosbiblioteca.utp.edu.co/tesisd/index.html>*

*Dedicado a
mis padres.*

Acknowledgments

My first debt of thanks goes to my supervisor Professor Alejandro Garcés at the Technological University of Pereira. For his support as advisor in this research and learning process, to promote in my career achievements such as the internship in Norway at the Norwegian University of Science (NTNU), where I had the opportunity to work in a great team of researchers at the cybernetics department under the supervision of Professor Marta Molinas.

I will also thank to Professor Marta Molinas for such enriching experience at NTNU, where I could learn not only English, but other subjects related to my research area. For her advice and great ideas regarding my project.

I am also grateful to my parents for supporting me unconditionally throughout this process to achieve my goals.

Special thanks to all my friends in Pereira and Trondheim for their support and assistance throughout this process, to cheer me up and help me in some way or another, or contributed their bit along this way.

I will also like to thank to SIRIUS research group, from which I could become part of it, for their support and friendship.

Abstract

This research work is aimed at the understanding and stability analysis of the control schemes for single phase converters and the phase locked loop (PLL), with the purpose to identify the impact of such approaches on the dynamics of the conversion system. A system consisting of a single phase voltage source converter (SP-VSC) with equivalent grid interconnection and source representation is designed in SIMULINK/MATLAB software using the average model of the converter. The control technique based on the well-established concept of vector control is explained, implemented and compared with other control techniques. The main task of the master thesis is oriented towards the stability analysis of the single phase converters within the two classical control strategies, voltage oriented control and proportional resonant control. Finally, a proposed control algorithm is applied to the SP-VSC, this based on Lyapunov theory, which fulfills the stability properties of a system.

Resumen

Este trabajo de investigación está dirigido a la comprensión y análisis de estabilidad de los esquemas de control para convertidores monofásicos y el Phase Locked loop (PLL), con el objetivo de identificar el impacto de dichos enfoques en la dinámica del sistema de conversión. Se diseña un sistema que consiste en un convertidor de fuente de voltaje monofásico (SP-VSC) interconectado a la red, en el software SIMULINK / MATLAB utilizando el modelo promediado del convertidor. Se explica una técnica de control clásico basada en el concepto de control de vectorial, además se implementa y compara con otras técnicas de control. El objetivo principal de esta tesis de maestría está orientada hacia el análisis de estabilidad de los convertidores monofásicos dentro de dos estrategias de control clásicas, control vectorial y control proporcional resonante. Finalmente, se propone una técnica de control y se aplica al SP-VSC, éste se basa en la teoría de Lyapunov, que cumple las propiedades de estabilidad de un sistema.

Table of Contents

Acknowledgments	iii
1 Introduction	1
1.1 Problem Description	1
1.2 Motivation for Research	2
1.3 Objectives of the Study	3
1.3.1 General	3
1.3.2 Specifics	3
1.4 Background	4
1.5 Control of the VSC	5
1.6 Main Results	7
1.7 Structure of the Thesis	7
2 Grid Synchronization	9
2.1 Phase locked loop (PLL)	9
2.1.1 Synchronous reference frame (SRF)	10
2.1.2 Single phase PLLs	11
2.2 Results	15
2.3 Summary of the chapter	19
3 Control techniques for single phase VSC	21
3.1 Voltage Oriented Control (VOC)	22
3.2 Resonant Control	24
3.3 Results	25
3.4 Summary of the chapter	29

<i>TABLE OF CONTENTS</i>	vii
4 Stability analysis	31
4.1 Results	37
4.2 Summary of the Chapter	42
Conclusions	43
A Lyapunov based control for SPVSC	45
A.1 Averaging	47

Chapter 1

Introduction

1.1 Problem Description

Recent interest in generating clean energy by using renewable resources, such as photovoltaic and wind energy, has emerged as a solution to deal with a highly variable power system. This type of generation units can be integrated under the concept of microgrid, which increases reliability and efficiency of the system. A microgrid is composed by integrating energy storage devices (such as batteries or flywheels), loads and distributed energy resources (DERs) interfaced by power electronic devices, usually a voltage source converter (VSC).

Efficient power generation from renewable energy source is highly dependant on the efficiency of the power electronics converter. Hence its controller is expected to be designed adequately to guarantee the proper regulation of its output power in all operating conditions.

In three phase systems the control techniques for VSC are generally based on the synchronous reference frame, since its transformation leads to constant variables. Therefore linear controllers are easily implemented, such as PI, which are designed to achieve zero steady state error by tracking a constant reference. On the other hand VSCs, have been widely used in single phase applications, e.g. in interfacing distributed generation to the Microgrid.

Single phase power systems or unbalanced three-phase systems are quite complex compared to conventional three-phase systems, this is due to the double frequency present in the instantaneous power, and from the point of view of the controller, the traditional PI controller is not able to achieve zero steady state for tracking a sinusoidal signal, because of the

integral term that is unable to track the reference of sinusoidal input [1]. That is the reason why conventional techniques require frame transformation from abc to $0dq$, which is the case of the controllers for three phase system in quadrature frame. In addition, the nonlinear nature of the conversion systems (due to the switching devices) increases the complexity of such systems, this will be explained later on, in Chapter 3 and particularly in Equations 3.1 and 1.4.

In grid connected systems the synchronization of a system becomes a crucial part of any control technique. Synchronization techniques have been used to accurately identify the phase angle and frequency of the grid voltage instantaneously, which simplify the controller design in the VSC. The *PLL* (*Phase Locked Loop*) is the most common method for this labor. Hence it becomes in a essential part of the control system specially in quadrature transformation based systems. Nevertheless, the reliance on PLL for developing the controller makes the system dependent on the controller tuning, which reduces the robustness of the system and deteriorates the dynamic response [2].

The stability analysis is essential to design a controller, however for single phase applications, as mentioned before, it becomes a more complex task, since its model is non linear. Existing methods can be categorized into frequency and time-domain methods. Nevertheless, the most popular type of studies are linearized approaches, that is the case of the small-signal impedance-based stability criterion.

It is important to establish the stability properties of any system, specially for control approaches. And, in order to consider the dynamics of the non linear system without relaxing the model by linearizing around a operational point a non linear stability analysis is needed for studying such non linear system. Thus, to obtain a more general conclusion of a technique, no matter the operational point.

1.2 Motivation for Research

Converters play a key role in interconnecting distributed energy resources within the microgrid. Its proper operation is expected to be designed adequately so all the energy capacity from renewable resources can be delivered to the grid.

The existing methodologies for the single phase converter adapt control techniques which are designed based on three phase converters. These methods include quadrature transfor-

mation, such as the synchronous ($0dq$) or the stationary reference frame ($\alpha\beta$). Thus another technique is to linearize the system around the steady-state point, therefore these controllers are suitable when the converter operates within the fixed operating points and the variation of system parameters and disturbances are small [3].

The classic control techniques use a PLL to synchronize the converter to the power grid. This synchronization methodology is the most common technique due to its easy implementation, however few researches have focused on the its impact on the stability. Specially when its role is as essential as monitoring the phase and frequency of the electrical grid. On the other hand, the PLL operates efficiently in optimal conditions, but any perturbation on the voltage grid makes it work misguidedly and lead to a wrong control operation. Hence, the stability might be affected in such way that it can cause the controller to fail and therefore the system to activate its protection system and disconnect.

This project proposes an stability analysis of the classic control methodologies on the single phase converters for microgrid applications, considering the impact of the PLL.

1.3 Objectives of the Study

1.3.1 General

The main objective of the project is to investigate and analyze the operation of single phase converters considering the impact of the PLL in microgrids applications.

1.3.2 Specifics

- To study single phase microgrids, phase locked loop, single phase voltage source converters.
- To model the single phase converter for microgrids applications.
- To implement at least three different PLL models in Matlab and compare them.
- To develop an understanding of the most common control strategy for VSC, the vector control technique.
- To analyze the stability of the designed control by Lyapunov criterion.
- To optimize the designed control performance.

1.4 Background

The single phase voltage source converters SP-VSC have been widely used in the recent years in various applications, such as uninterruptable power supplies (UPSs) [4], active filters [5], power factor correction circuits [6]; and for interfacing new technologies such as distributed generation [7] and electric vehicles batteries [8], among others [9], [10].

Pulse With Modulation (PWM) based SP-VSC has been a subject of research for many years moreover the most common technique mainly for power factor correction [11], which is one of the objectives of the VSC as rectifier. The power factor close to unity avoid any additional compensation since there is no reactive power injection [12]. To achieve this objective the ac side current (i_{ac}) should be in phase with the voltage grid (V_s), [13].

Several control techniques have been developed in order to design a proper control for the single phase converters, which can be classified in two control types: Direct Power Control (DPC) and Current Control (CC).

The direct power control is based on instantaneous power theory, also known as p-q theory, and it's been based mainly in digital control, such as model predictive control (MPC) [14], deadbeat [15], repetitive [16], fuzzy logic lookup table [17] y sliding mode control [18]. Despite the advantages these methodologies offer, they have some drawbacks such as complexity in the design, sensibility to variation in the parameters and steady state errors [19].

The current control techniques have been widely used in single phase converters. Among the most popular methodologies the current hysteresis control (CHC), PI based control, such as “*Voltage oriented control*” (VOC) [20], Proportional Resonant (P-R) and Lyapunov current control [21]. Current hysteresis control is based on the instantaneous current error, which is one of the most used techniques due to its precision and simplicity [22]. However these current control techniques tend to depend on the system parameters and the operational conditions of the converter [23].

The design of several methodologies above mentioned are based either on the synchronous reference frame (SRF “d-q”) or the stationary reference frame ($\alpha\beta$). Both transformations imply quadrature signals, therefore in single phase systems it is required to generate a fictitious quadrature signal. To achieve this there have been diverse proposals e.g. [20], in which the VOC is based on a new method to generate such fictitious axis.

In addition, most of the proposed techniques are based on the PLL or any other technique to synchronize with the grid [24]. But the most common is the PLL since its implementation is easy and simple, besides it has proved to be efficient and robust. The angle derived from the PLL is used to perform the shift to other reference frames and hence develop a adequate controller for single phase converters, this process is identical to the control design for three phase systems.

Other researches have been interested on developing methodologies to achieve unity power factor directly in the abc reference frame [6, 10, 25, 26]. Which are simple and easy to implement according to [12]. However the PLL is essential in this type of controllers, and those who are not based on the PLL, design digital controllers in order to deal with the unavoidable nonlinearities of the model from the single phase converter.

1.5 Control of the VSC

The Voltage Source Converter plays an important role in converting the energy, since it is the integrator element between the distributed generation and the grid, in this specific case from DC to AC systems, as a inverter. It is composed by semiconductor devices like insulated gate bipolar transistors (IGBT) gate-turn-off thyristors (GTOs), or integrated gate controlled thyristors (IGCTs), with antiparallel diodes to produce a controlled dc voltage. The IGBTs are controlled to switch efficiently in order to guarantee the proper operation of the converter. The most common technique for switching the devices is based on PWM (“pulse with modulation”) which generates a modulated signal by comparing the instantaneous magnitude of a triangular waveform with sinusoidal input reference. Therefore the VSC is operated in such way that its output is a desired and controlled signal [27].

This document focuses on the synchronization and the current control of single phase converters. Fig. 1.1 shows a scheme of a single phase converter for grid connected applications whose mathematical model will be described in Chapter 3. Figure 1.1 is showing, for instance a photovoltaic panel interfaced by a VSC to the power grid. And in order to achieve a proper operation of such configuration, the first stage will be to synchronize to the grid to be able to interconnect them, this information will be sent to the control stage, in which the strategy is to develop a modulated signal such that the PWM will produce the switching signals for the voltage source converter.

To be more precise and to control properly the switching devices to adequately manage the power transfer, it is necessary to develop a control strategy which can overcome this purpose. Such control must consider the synchronization to the power grid, since it is interfacing dis-

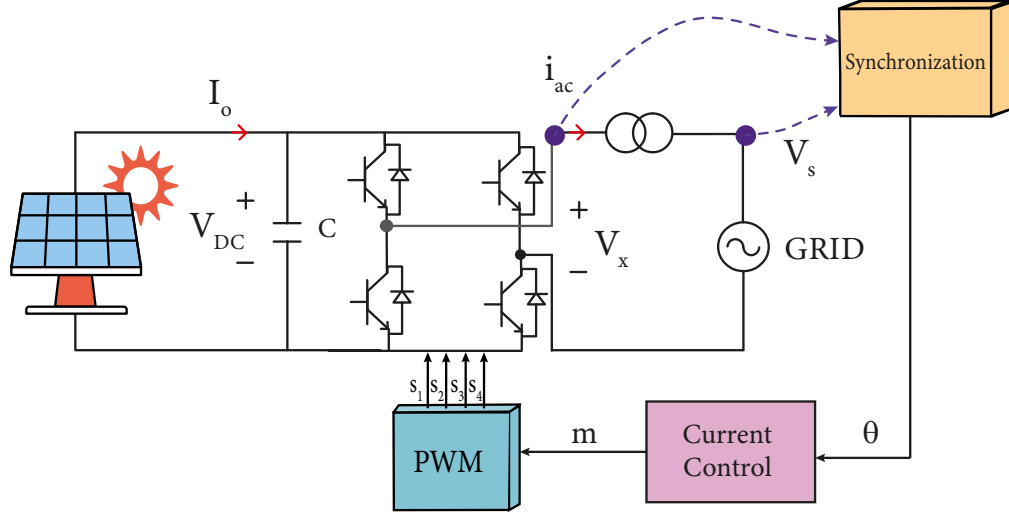


Figure 1.1: Single Phase Converter interfaced to the power grid

tributed energy resources to the grid. Furthermore, the controller needs to consider within its implementation the phase angle and the frequency of the grid, therefore the synchronization is quite an important part of this approach.

1.6 Main Results

This study has three main contributions as follows:

- The synchronization issue is studied and particularly for single phase converters four different type of orthogonal signal generators are compared. The best performance of the synchronization techniques is used into the control approaches exposed in this work.
- Two classical control techniques are studied and also compared, the vector control based on the synchronous reference frame and the proportional resonant control based on the stationary reference frame. From here one of the topologies is chosen to analyze its stability properties.
- A stability analysis is accomplished over a control technique, the results show a stable region to select the values of the controller parameters k_p and k_i . This is achieved by Lyapunov theory and simulation analysis.

1.7 Structure of the Thesis

The main objective of this thesis is based in two principal elements of the control scheme presented already in Fig. 1.1, namely the grid synchronization and the current control. Four types of orthogonal signal generators for the synchronization issue were studied and evaluated in terms of performance in Chapter 2. The technique with the best performance is selected to apply it within the controllers. In Chapter 3, two classical control strategies for single phase voltage source converters are evaluated. Furthermore, the best control with the best synchronization scheme are rigorously analyzed based on Lyapunov stability theorems, this is explained in Chapter 4. Finally, as a result of this work, a new control is proposed, in which the dynamics of the system are considered, this is exposed as an extension or future work and it is presented in Appendix A.

Due to the structure of the research, each chapter contains a result section from which its conclusions are summarized in another section. For better understanding, the structure of this thesis is shown in Fig. 1.2. From which each chapter is depicted by a rectangle containing the main features of it, for instance, Chapter 2 contains the derivative, integral, delay and SOGI approaches for PLL, this is represented as smaller rectangles named *Deriv*, *Int*, *Delay* and *SOGI* and the next chapter will involve the conclusions of the previous chapter. This means that Chapter 3 will implement the SOGI-PLL within its control strategies, the voltage oriented control depicted as *VOC* and the proportional resonant as *PR*.

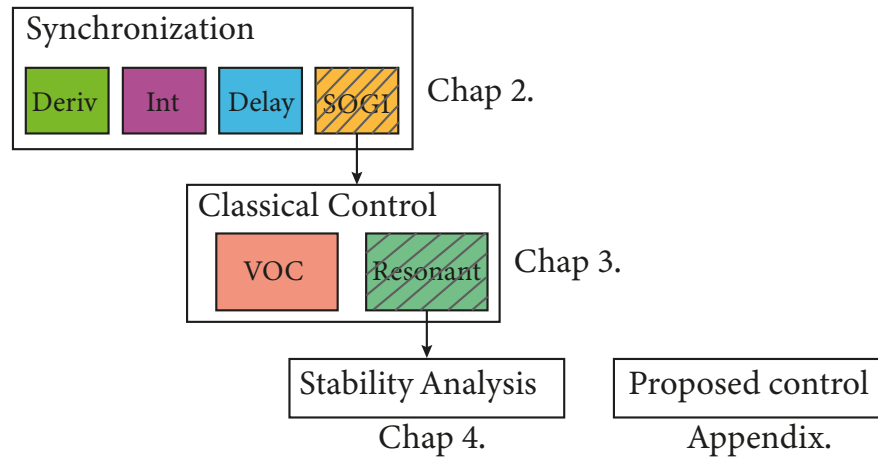


Figure 1.2: Structure of the thesis.

Chapter 2

Grid Synchronization

In this chapter the synchronization issues for single phase systems will be described along with basic concepts to understand its application to microgrids. Among them, the synchronous reference frame (SRF), which is used into the phase locked loop (PLL) to determine the phase angle to synchronize with the power grid. Thus, four types of quadrature signal generators are analyzed and compared to finally choose the best approach for synchronizing to the grid and to be applied into the controller.

2.1 Phase locked loop (PLL)

Any element interconnected to the power grid required to be synchronized, this means minimize the difference of phase, amplitude and frequency in the voltage between the power supply and the integrating element, which can be either a synchronous machine as in the conventional power system, or a new element such as distributed energy resources (DERs). Synchronizing is also very important to secure continuous and stable operation [28].

The synchronization in the electric power system becomes a challenge for the new technologies added to the grid, since they are usually power electronic based elements (non rotating elements), which means its control must be designed to consider the voltage variations in real time.

There are several methods in the literature to synchronize to the grid, such as zero crossing detection (ZCD), Kalman Filter, discrete Fourier transform (DFT), nonlinear least square (NLS), adaptive notch filtering (ANF), artificial intelligence (AI), delayed signal cancellation (DSC) , phase locked loop (PLL), and frequency locked loop (FLL) [24].

A simple and effective technique that is used to detect the phase angle is the Phase locked loop (PLL). It can be described as a “nonlinear closedloop feedback control system which synchronizes its output signal with the reference input signal in frequency and phase” [24]. Fig. 2.1, shows a basic PLL structure.

In this work the synchronous reference frame PLL (SRF-PLL) will be used for the control design. However, since we are focused on single phase systems from now on the single phase PLL and the control design will be described for these particular systems. The main challenge of single phase PLL is the generation of quadratic signal as will be described below.

2.1.1 Synchronous reference frame (SRF)

Synchronous reference frame is a shift in reference from abc to a quadrature frame denominated “ $0dq$ ”. This is applied in electrical machines to have a frame which rotates at a synchronous speed, usually ω depends on the electrical frequency of the system, which is the frequency to synchronize with. The transformation is developed in two steps, a transformation from a three phase system abc to a stationary coordinate system $\alpha\beta$, which is known as Clarke transformation, and a transformation from the $\alpha\beta$ stationary coordinate system to the $0dq$ rotating coordinate system, which is known as Park transformation.

Clarke transformation $abc \rightarrow \alpha\beta$ is represented by Equation 2.1

$$\begin{bmatrix} v_\alpha \\ v_\beta \end{bmatrix} = \sqrt{\frac{2}{3}} \begin{bmatrix} 1 & -\frac{1}{2} & -\frac{1}{2} \\ 0 & \frac{\sqrt{3}}{2} & -\frac{\sqrt{3}}{2} \end{bmatrix} \begin{bmatrix} v_a \\ v_b \\ v_c \end{bmatrix} \quad (2.1)$$

rotation $\alpha\beta \rightarrow 0dq$ is shown in Equation 2.2.

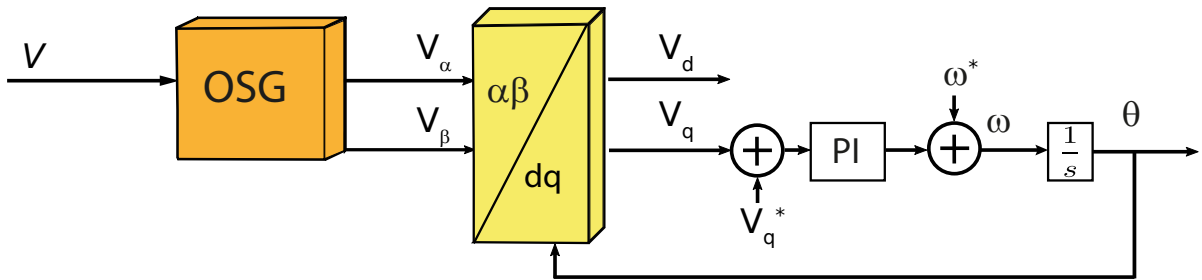


Figure 2.1: General PLL scheme.

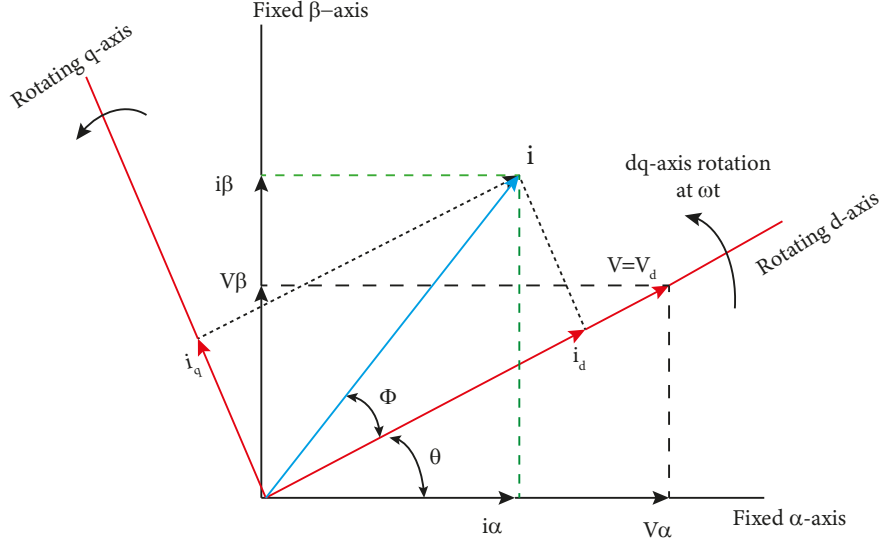


Figure 2.2: Park transform.

$$\begin{bmatrix} v_d \\ v_q \end{bmatrix} = \begin{bmatrix} \sin(\theta) & -\cos(\theta) \\ \cos(\theta) & \sin(\theta) \end{bmatrix} \begin{bmatrix} v_\alpha \\ v_\beta \end{bmatrix} \quad (2.2)$$

Park transformation $abc \rightarrow 0dq$ [29]:

$$\begin{bmatrix} v_0 \\ v_d \\ v_q \end{bmatrix} = \sqrt{\frac{2}{3}} \begin{bmatrix} \frac{1}{\sqrt{2}} & \frac{1}{\sqrt{2}} & \frac{1}{\sqrt{2}} \\ \cos \theta & \cos \left(\theta - \frac{2}{3}\pi \right) & \cos \left(\theta + \frac{2}{3}\pi \right) \\ \sin \theta & \sin \left(\theta - \frac{2}{3}\pi \right) & \sin \left(\theta + \frac{2}{3}\pi \right) \end{bmatrix} \begin{bmatrix} v_a \\ v_b \\ v_c \end{bmatrix} \quad (2.3)$$

It is important to notice that there are different types of Park and Clarke transformations. In this case we are considering the power invariant transformation which is usual in power system applications. Other types of transformations can be used without changing significantly the analysis.

2.1.2 Single phase PLLs

It is worth notice that for three phase systems the shift in reference is easily achieved, since it is possible to transform from abc to dq directly as in Equation 2.3. But for single phase systems there is only one measuring signal (e.g. phase a), therefore a fictitious axis β must be generated. There are several methods to do so [30], but in this document only the simplest

ones are developed with the aim of showing effectiveness of the controller. Hence, Park transformation is applied directly for single phase systems.

The fictitious axis β is obtained from phase shifting the measured signals by a quarter of the period by means of any orthogonal signal generation (OSG) method. Such as derivation, integration or simply delaying the measured signal. The second order generalized integrator (SOGI) is another kind of OSG, which has shown great results under different conditions and its easy implementation makes it suitable for single phase applications. Fig. 2.3 shows the above mentioned methods to generate the fictitious axis and Equations 2.7, 2.9, 2.11 and 2.13 describe mathematically the orthogonal signal generator by means of derivative, integral, delaying and SOGI approach respectively.

Notice that in the first three approaches (derivative, integral, delay) the frequency is established as a parameter, therefore if the frequency changes (which is already varying all the time around the fundamental frequency) these methods will not be able to operate under other circumstances different than the ideal operational frequency. The second order generalized integrator on the other hand, is designed to have the frequency not as a parameter but as an input, this is visible in the Fig. 2.3.d. Hence, this approach is consider to be more accurate than the other mentioned methods, since the frequency is a feedback from the PLL process.

To explain better, lets consider the following: if the input voltage of the PLL is given by:

$$v = V \sin(\theta) = V \sin(\omega t + \phi) \quad (2.4)$$

the output signals in stationary reference frame $\alpha\beta$ can be expressed by the following voltage vector:

$$\begin{bmatrix} v_\alpha \\ v_\beta \end{bmatrix} = V \begin{bmatrix} \sin(\theta) \\ -\cos(\theta) \end{bmatrix} \quad (2.5)$$

in here the following Equation describes the derivative approach to get the quadrature signal V_β .

$$V_\alpha = V \sin(\omega t + \phi) \quad (2.6)$$

$$\frac{dV_\alpha}{dt} = \omega V \cos(\omega t + \phi) \rightarrow V_\beta = -\frac{1}{\omega} \frac{dV_\alpha}{dt} \quad (2.7)$$

The integral approach is shown in the next Equation:

$$V_\alpha = V \sin(\omega t + \phi) \quad (2.8)$$

$$\int V_\alpha dt = -\frac{V}{\omega} \cos(\omega t + \phi) \rightarrow V_\beta = \omega \int V_\alpha dt \quad (2.9)$$

Delaying the input signal $V_s = V_\alpha$ simply means that the quadrature signal will be 1/4 of the fundamental period behind the original signal. For this particular case, when the frequency is consider to be around 60Hz, and also for the implementation, the delay is z^{-420} since the sampling period is $T_s = 1 \times 10^{-5}$, and the mathematical description of this can be expressed as:

$$V_\alpha = V \sin(\omega t + \phi) \quad (2.10)$$

$$V_\beta = V \sin\left(\omega t + \phi - \frac{T}{4}\right) = V \cos(\omega t + \phi) \quad (2.11)$$

The differential equation of the SOGI approach is presented as follows:

$$\frac{dV_\alpha}{dt} = \omega (K (V_s - V_\alpha) - V_\beta) \quad (2.12)$$

$$\frac{dV_\beta}{dt} = \omega V_\alpha \quad (2.13)$$

where $K = \sqrt{2}$ [31].

However, the most common representation to describe this method is through the transfer function [32] as shown below:

$$\frac{V_\alpha}{V_a} = \frac{K \cdot \omega' \cdot s}{s^2 + K \cdot \omega' \cdot s + \omega'^2} \quad (2.14)$$

$$\frac{V_\beta}{V_a} = \frac{K \cdot \omega'^2 \cdot s}{s^2 + K \cdot \omega' \cdot s + \omega'^2} \quad (2.15)$$

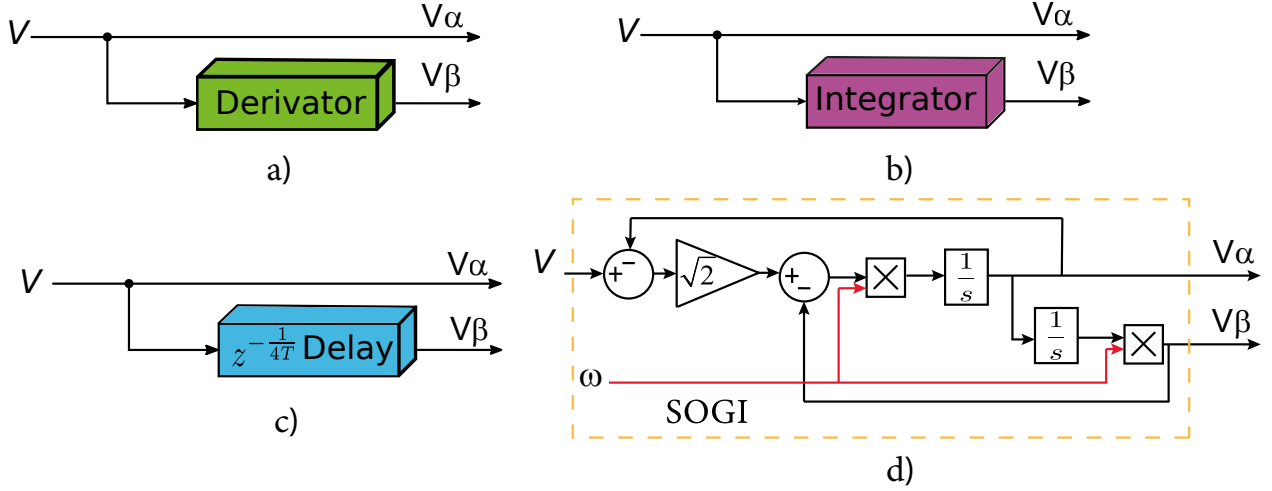


Figure 2.3: Different OSG for Single Phase PLL. a) Derivator, b) Integrator, c) Delay, d) SOGI

where ω' is the resonance frequency, since this method is based on the properties of the proportional-resonant controller (which will be explained in Chapter 3) to eliminate steady state error at such frequency [33].

After generating the imaginary axis the synchronization is held by the phase locked loop (PLL) as is observed in Fig. 2.4. Where the objective is to detect and identify the grid voltage angle, thus, this angle θ is sent as feedback to be used in Park's transformation.

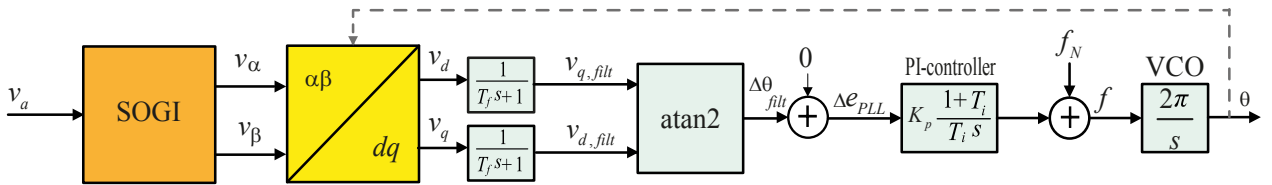


Figure 2.4: Single Phase PLL-SOGI based.

The configuration showed in Fig. 2.4 is not a product of this work, interested readers can refer to the following article [34]. Although the application in this reference is for three phase systems, the PLL proposed structure is considering the pre-loop filter and it is applicable to single phase systems.

2.2 Results

This section is dedicated to show the performance of four different types of quadrature signal generators as described above. In order to be more specific, the implementation in SIMULINK/MATLAB of the mentioned approaches is also shown. Thus, a simple test will show how they behave under the same conditions. This with the purpose of compare them and get some conclusions.

The application of the mentioned approaches for generating the quadrature signal V_β are shown in Fig. 2.5 and 2.6, where Fig. 2.5 contains the derivative, integral and delay approaches, which are quite easy to implement. It is important to remember that the frequency in these methodologies comes as a constant parameter (60Hz) pre-multiplied in the derivative and integral approaches as shown in Fig. 2.5. The implementation of the second order general integrator is shown in Fig. 2.6, where $K = \sqrt{2}$ as mentioned before, in here the frequency comes out from the PLL as an input to this system, therefore we expect it to behave better under frequency changes.

The complete implementation of the single phase PLL based on the SOGI is shown in Fig. 2.7. The same goes with the other approaches, in here we show only one of them for simplicity.

The behavior of the OSG-PLL approaches is presented in Fig. 2.8 and Fig. 2.9, in both figures a frequency step of 5Hz (60 – 65 Hz) and an amplitude step (1pu -1.2pu) is affecting the voltage grid at the second 0.56s. Hence, Fig. 2.8 depicts the quadrature signal generation, this means $\alpha - \beta$ from each OSG method, from which it can be observed that all of them synchronize properly before the step at 0.56s and the quadrature signal is generated as it should be. However, after the frequency and amplitude step it seems like some of them manage to work properly again, but that is not the case for the derivative and the integral method, since in the first one, the generated V_β can not reach the same amplitude of the original signal V_a and in the second one is the opposite, V_β has larger amplitude than V_a . Therefore, from Fig. 2.8 the approaches that can stabilize after the changes are the SOGI and the delay.

In order to confirm the mentioned result, Fig. 2.9 presents the behavior of the frequency ω for each OSG-PLL, under the same conditions as said before, moreover, it can be observed the synchronization of the analyzed PLLs. From this figure it is noticeable that although in the previous figure the integral method show a great quadrature signal generation, ω seems to be out of range, since it has an oscillatory behavior the entire time. Furthermore, the derivative

approach after the change definitely does not manage to stabilize, this verifies the above conclusion regarding the derivative-PLL. However the Delay-PLL does not synchronizes after the contingency and this is not visible in the quadrature signal (Fig. 2.8) but it is evident in this figure (Fig. 2.9). Finally it is worth notice that the SOGI-PLL is the only one which can reach the new frequency and amplitude and manage to stabilizes quickly, this should be due to the frequency feedback from the PLL, additionally this conclusion is validated by both figures.

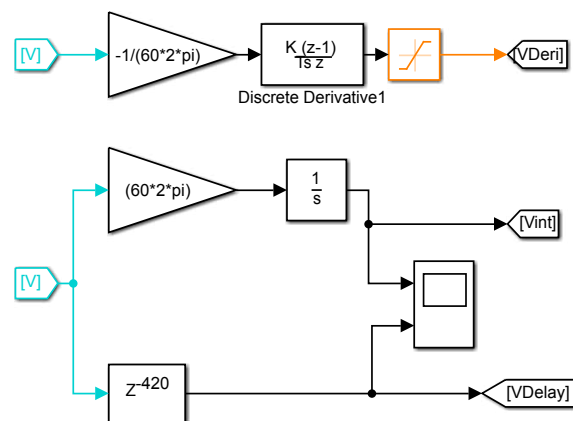


Figure 2.5: Implemented Derivative, integral and Delay approach.

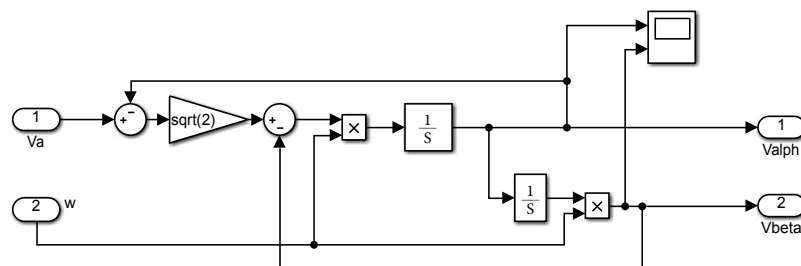


Figure 2.6: Implemented Second-order generalized integrator (SOGI).

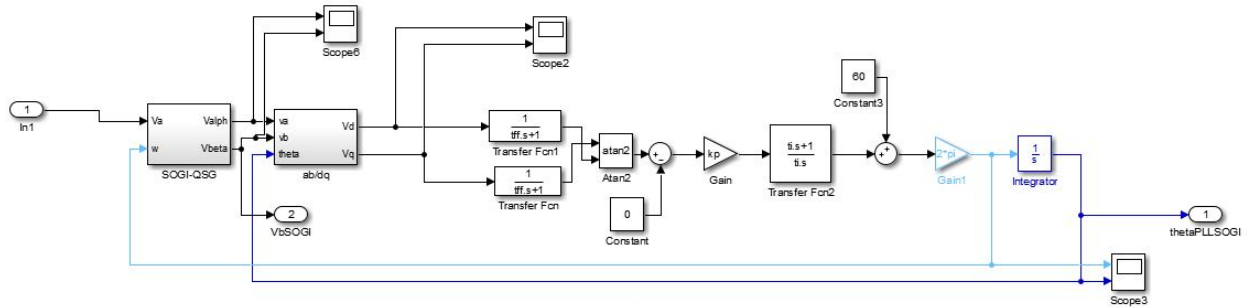


Figure 2.7: Second-order generalized integrator (SOGI) based phase-locked loops (PLLs) .

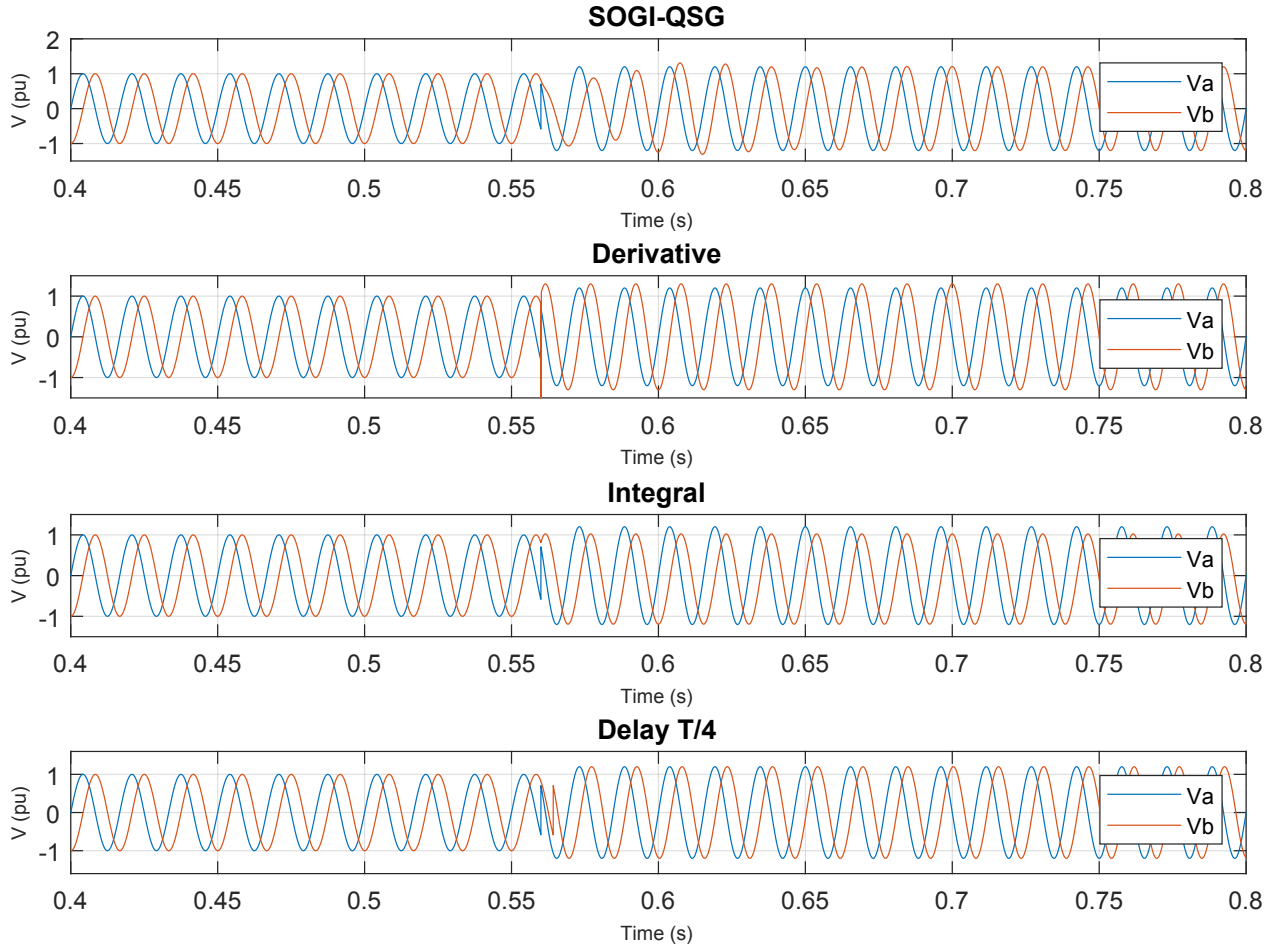


Figure 2.8: Quadrature signals with frequency step (60-65 Hz) and amplitude step (1pu -1.2pu) at 0.56s.

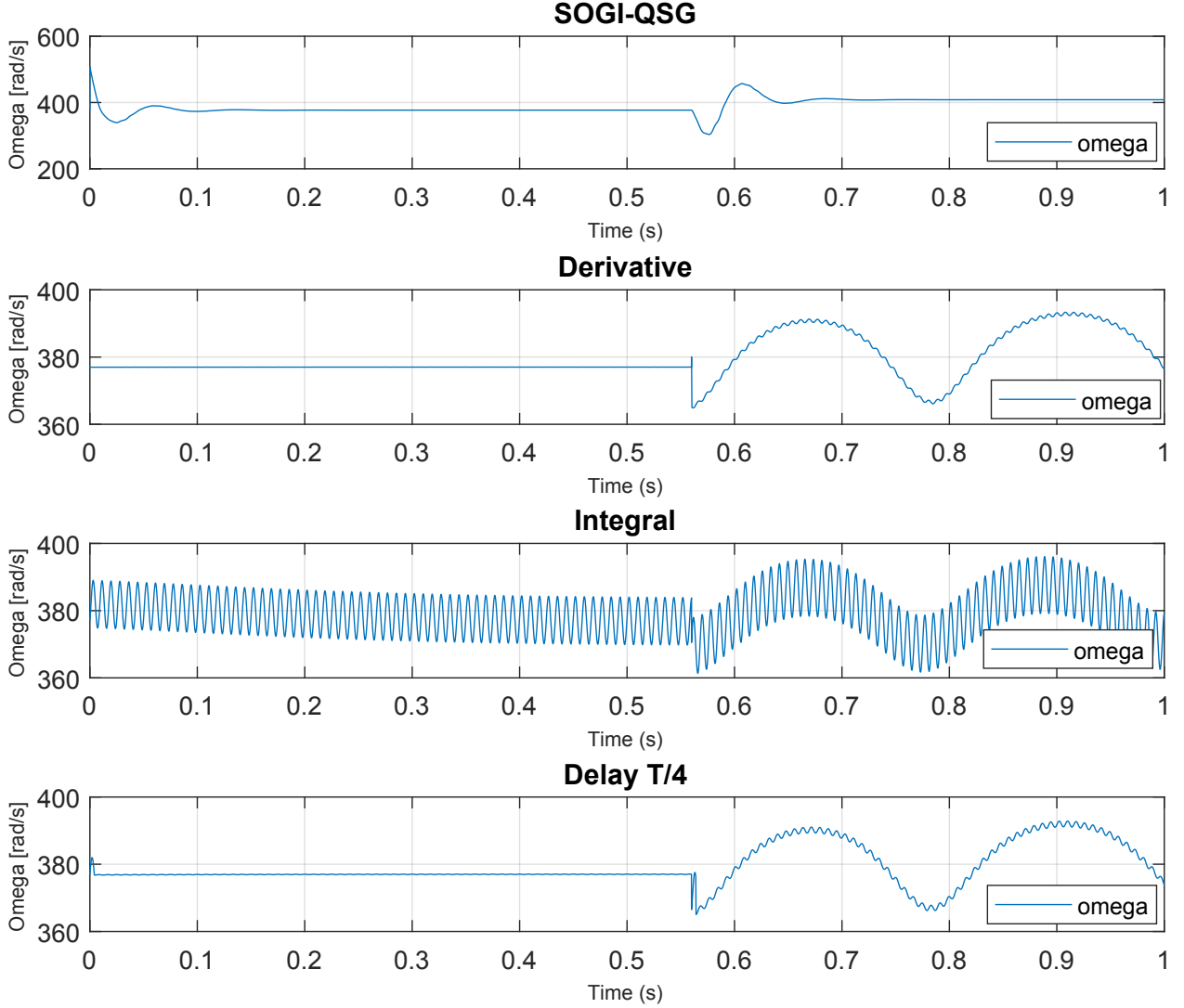


Figure 2.9: Omega with frequency step (60-65 Hz) and amplitude step (1pu -1.2pu) at 0.56s.

2.3 Summary of the chapter

Through this Chapter the synchronization issue is exposed and specially for single phase systems connected to the grid. It is relevant to mention that although single phase systems seem to be a simplification of three phase systems on the contrary it is more complicated

for example to apply directly the frame transformations, since it only has one measurement signal. However, there are some approaches adapted for single phase, for instance, the OSGs also discussed in this Chapter. In which four approaches, derivative, integral, delay and SOGI were explained. The PLL along with these OSG methods were implemented in SIMULINK/MATLAB software and they were compared to show their behavior under some circumstances. From the results we can conclude that the SOGI-PLL shows better results in comparison with the other approaches and therefore this configuration will be used from now on for further analysis.

It is important to notice that non of these OSG neither the PLL are linear approaches, it seems like its components are simple, but the model is quite complicated and moreover is non linear. It have been transformed to the frequency domain by some assumptions but this only with the purpose of applying the techniques in real implementation. Furthermore, considering the non-linearities makes the analysis even more difficult.

Chapter 3

Control techniques for single phase VSC

The control techniques described in this chapter will be developed using the results from the previous chapter, in which the Second Order General Integrator Phase Locked Loop (SOGI-PLL) presented a better performance in contrast with three other simple techniques. Fig. 3.1 shows the typical configuration for controlling power converters. In this chapter two different control techniques will be described and compared for single phase applications. Voltage Oriented Control, a well known technique in the synchronous reference frame PI based, and Resonant control which is developed in the stationary reference frame.

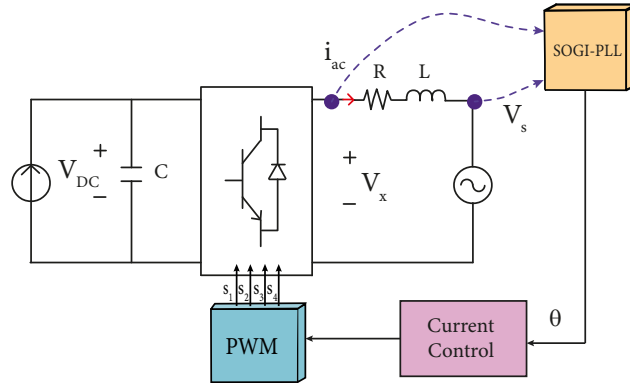


Figure 3.1: Typical current control for VSC.

From Fig. 3.1 the following equation describes the system dynamics of the *ac* side.

$$V_x = i_{ac}R + L\frac{di_{ac}}{dt} + V_s(t) \quad (3.1)$$

where:

- $V_x = mV_{DC}$ is the VSC output voltage.
- i_{ac} is the current in the AC side.
- L and R are the inductor and its resistance

Also, $V_s(t)$ is the grid voltage of the form $V_s = A \cdot \cos(\omega t + \phi)$, which is T- periodic function. Notice that the time is explicitly in this equation, therefore the system is time dependent, with the dynamics of the *dc* side given by:

$$\frac{P}{V_{DC}} = C\frac{dV_{DC}}{dt} + I_{DC} \quad (3.2)$$

It is assumed that the switching frequency is high and also the converter is a loss-less system, therefore

$$P_{ac} = P_{DC}$$

$$V_x i_{ac} = V_{DC} I_{DC}$$

average model:

$$mV_{DC} = V_x$$

$$I_{DC} = \frac{V_x i_{ac}}{V_{DC}} = m i_{ac} \quad (3.3)$$

Equation 1.2 becomes

$$P = \frac{C}{2} \frac{dV_{DC}^2}{dt} + mV_{DC} i_{ac} \quad (3.4)$$

3.1 Voltage Oriented Control (VOC)

Voltage Oriented Control is a classical control technique used in VSC converters due to its simplicity on implementation. It is a control based on the synchronous reference frame (dq) so the system must be shifted to this new reference. A proper definition from [35] says: “If the dq frame is oriented such that the d axis is aligned on the grid voltage vector, the control is called voltage oriented control (VOC)”. This technique is being widely used both in three phase systems and single phase systems, especially when the OSG has already been established to emulate beta, and similar to three-phase systems, the same procedure is applied for single phase power converters. It is worth notice that the control objectives mentioned in this chapter are focused on the inner loop, mainly known as the current control. Fig. 3.2 shows the general scheme of this approach.

From Equation 3.1 and using $0dq$ transformation we get:

$$V_x = i_{ac}R + L \frac{di_{ac}}{dt} + V_s(t) \quad (3.5)$$

$$\begin{bmatrix} V_{xd} \\ V_{xq} \end{bmatrix} = R \begin{bmatrix} i_d \\ i_q \end{bmatrix} + L \frac{d}{dt} \begin{bmatrix} i_d \\ i_q \end{bmatrix} + L \begin{bmatrix} 0 & -\omega \\ \omega & 0 \end{bmatrix} \begin{bmatrix} i_d \\ i_q \end{bmatrix} + \begin{bmatrix} V_{sd} \\ V_{sq} \end{bmatrix} \quad (3.6)$$

and rewriting

$$\frac{d}{dt} \begin{bmatrix} i_d \\ i_q \end{bmatrix} = \begin{bmatrix} -R/L & \omega \\ -\omega & -R/L \end{bmatrix} \begin{bmatrix} i_d \\ i_q \end{bmatrix} + \begin{bmatrix} 1/L & 0 \\ 0 & 1/L \end{bmatrix} \begin{bmatrix} V_{xd} \\ V_{xq} \end{bmatrix} + \begin{bmatrix} -1/L & 0 \\ 0 & -1/L \end{bmatrix} \begin{bmatrix} V_{sd} \\ V_{sq} \end{bmatrix} \quad (3.7)$$

which can be also seen as a linear system if V_{dc} is considered as constant, since the modulation index for the pulse with modulation interrelate the voltage from the ac and the dc side $m = \frac{V_x}{V_{DC}}$.

$$\frac{d}{dt} \begin{bmatrix} i_d \\ i_q \end{bmatrix} = \begin{bmatrix} -R/L & \omega \\ -\omega & -R/L \end{bmatrix} \begin{bmatrix} i_d \\ i_q \end{bmatrix} + \begin{bmatrix} V_{DC}/L & 0 \\ 0 & V_{DC}/L \end{bmatrix} \begin{bmatrix} m_d \\ m_q \end{bmatrix} + \begin{bmatrix} -1/L & 0 \\ 0 & -1/L \end{bmatrix} \begin{bmatrix} V_{sd} \\ V_{sq} \end{bmatrix} \quad (3.8)$$

Writing the equation in the form 3.6 and considering V_{DC} as constant, the system is clearly linear.

$$\frac{di}{dt} = A \cdot i + B \cdot m + C \cdot V_s \quad (3.9)$$

Hence, the typical PI controller for three phase is proposed also for single phase converters [36], [37], as in [23] where they present an analysis of the unbalanced SRF current control



where:

- I_d^*, I_q^* represent the reference current for both d and q axis.
- Vd, Vq, Id, Iq are the voltage and current measured from the circuit after $\alpha\beta - dq$ transform.
- θ is the angle obtained from the PLL.

An advantage of this approach is that since PI control is a well proven methodology, the application to single phase only will require an adequate OSG to create a fictitious axis and therefore use the synchronous reference frame as for three phase systems. This makes simpler the implementation of the VOC and in general it has been giving good results. However, PI controllers are unable to track a sinusoidal reference without steady-state error that is the reason for the axis transformation [35]. But for single phase applications and to avoid using axis transformation, there are other methodologies which operate directly in the stationary reference frame, that is the case of the Proportional-Resonant control. This control will be explained in the next section.

3.2 Resonant Control

The main idea behind proportional resonant control is to track an oscillating signal at a resonant frequency by introducing an infinite gain at a selected frequency for eliminating steady state error at such frequency [33]. Ideally the PR controller will have an infinite gain at the resonant frequency (60Hz) and the transfer function of the PR will be of the form of Equation 3.7. An advantage of this idea is to avoid the use of frame transformation as in the VOC method, which is guaranteed by including the disturbance (V_s) in the model within the controller in order to ensure perfect rejection [35]. This approach can be directly applied to single phase systems, since this control is applied in the ac reference frame, and therefore the dynamical system is non-autonomous. The basic proportional-resonant current control for a single-phase converter is depicted in Fig 3.3.

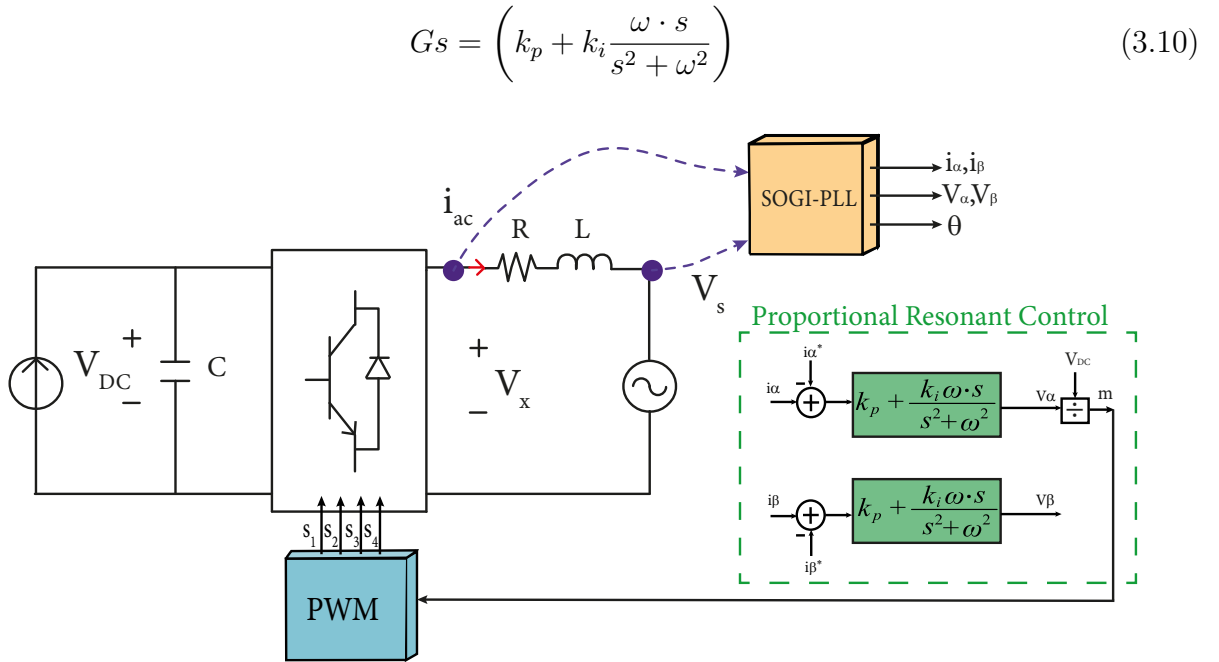


Figure 3.3: Proportional Resonant based current control.

For better understanding Equations 3.8, 3.9 and 3.10 will describe the methodology.

$$(I_{ref} - I_s) \underbrace{\left(k_p + k_i \frac{\omega \cdot s}{s^2 + \omega^2} \right)}_{\hat{z}} = m V_{DC} = V_x \quad (3.11)$$

It is important to get a more general description of the model, to do that, the transfer function will be transformed into a state representation using the observable canonical form.

$$\dot{z} = \begin{pmatrix} 0 & 1 \\ -\omega^2 & 0 \end{pmatrix} z + k_i \omega (I_{ref} - i_s) \quad (3.12)$$

$$mV_{DC} = z_1 + K_p (I_{ref} - i_s) \quad I_{ref} = I_{ref}(f_{PLL}) \quad (3.13)$$

It can be observed, comparing Fig. 3.2 and Fig. 3.3, that the complexity of the calculations has been significantly reduced as there is no need for the axis transformation and the cross-coupling terms [35].

3.3 Results

This section is dedicated to compare the two methodologies exposed previously in this chapter. Such controllers were implemented in SIMULINK/MATLAB software, using the conclusions from the former chapter, the SOGI-PLL was added as a synchronizer to these models. Thus, the current control is tested by changing the reference, both methods were developed under the same conditions. This with the purpose of compare them and get some conclusions.

The study case is exposed by Fig. 3.4, the values were taken from [39] and it was implemented for both methods, which are shown in Fig. 3.5 and Fig. 3.6. Where Fig.3.5 presents the voltage oriented control with $K_p = 10$ and $K_i = 30$ and Fig. 3.6 depicts the proportional resonant control in which the proportional constant is $K_p = 0.04$ and the integral constant equal to $K_i = 1$. It is important to remember that the tuning of the controller parameters can be done by many different technique and depending on the value of these parameters the controller will operate in diverse results. Moreover the mentioned parameters will also have to be re-tuned if there is a change in parameters of the system.

The current control is expect to track a reference signal, which is set to be a step signal from 2A to 8A. The result from VOC technique is shown in Fig. 3.7 from which it can be observed that the control manage to track the reference signal despite the step at the second 1s. However, the current signal as a result of the switching devices presents oscillatory behavior. Fig. 3.8 presents the result from P-R current control in which it can be notice that the current signal follows the reference even after the change in it. The more straight forward difference between both approaches is the reference frame from each of them, the

P-R is a methodology design to track an oscillating signal at a resonance frequency, therefore as a result we can observe a sinusoidal signal as a reference and how this control tracks it with high accuracy.

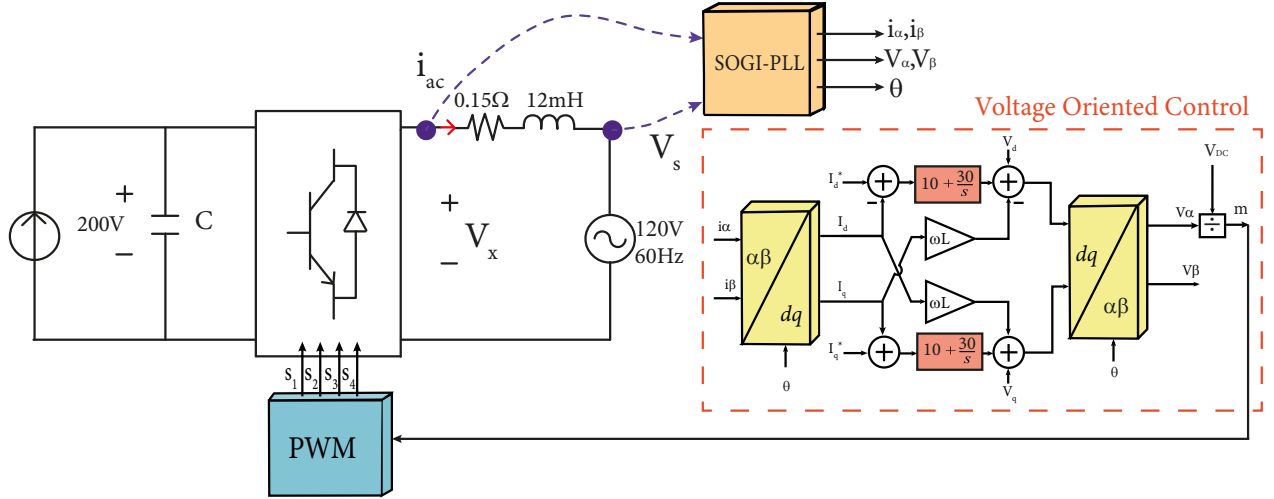


Figure 3.4: Study case of VOC applied to single phase converter (SPC).

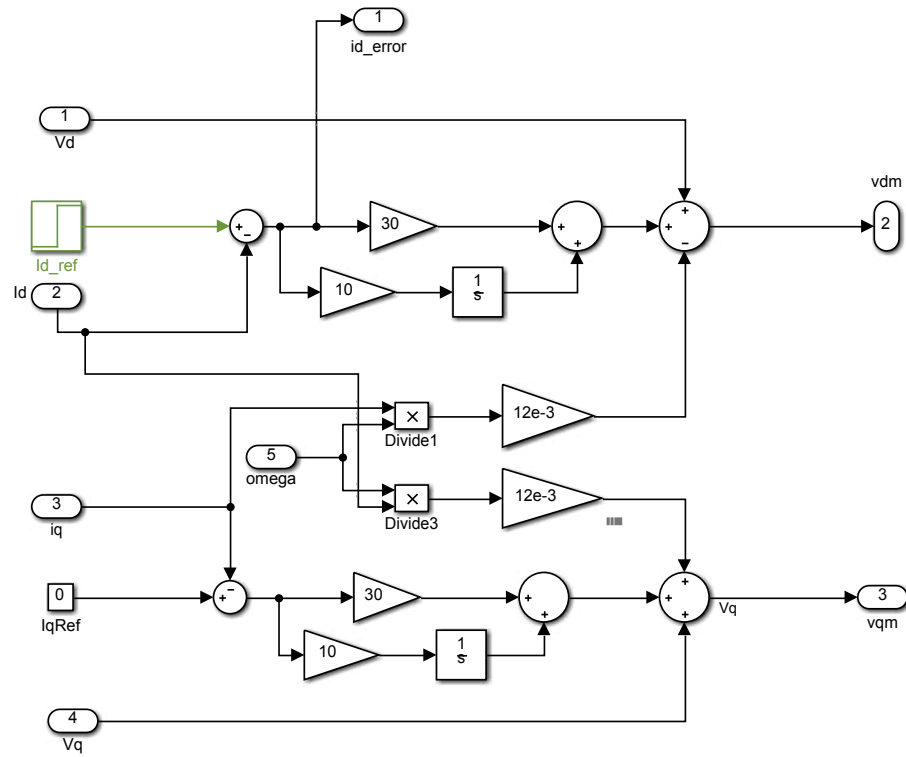


Figure 3.5: SPC VOC SIMULINK/MATLAB implementation.

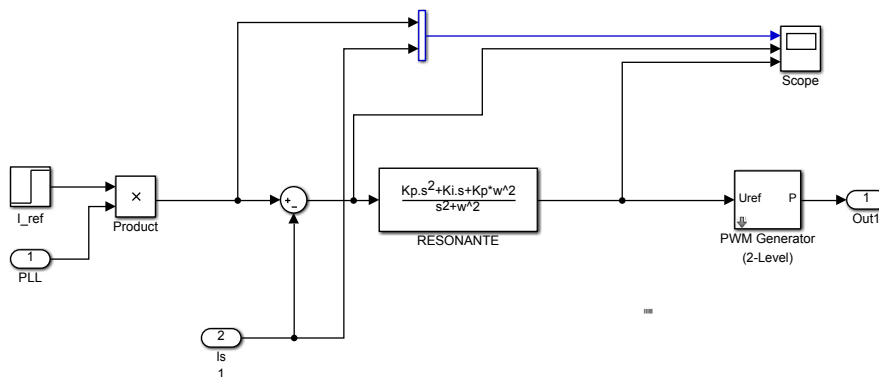


Figure 3.6: SPC PR SIMULINK/MATLAB implementation.

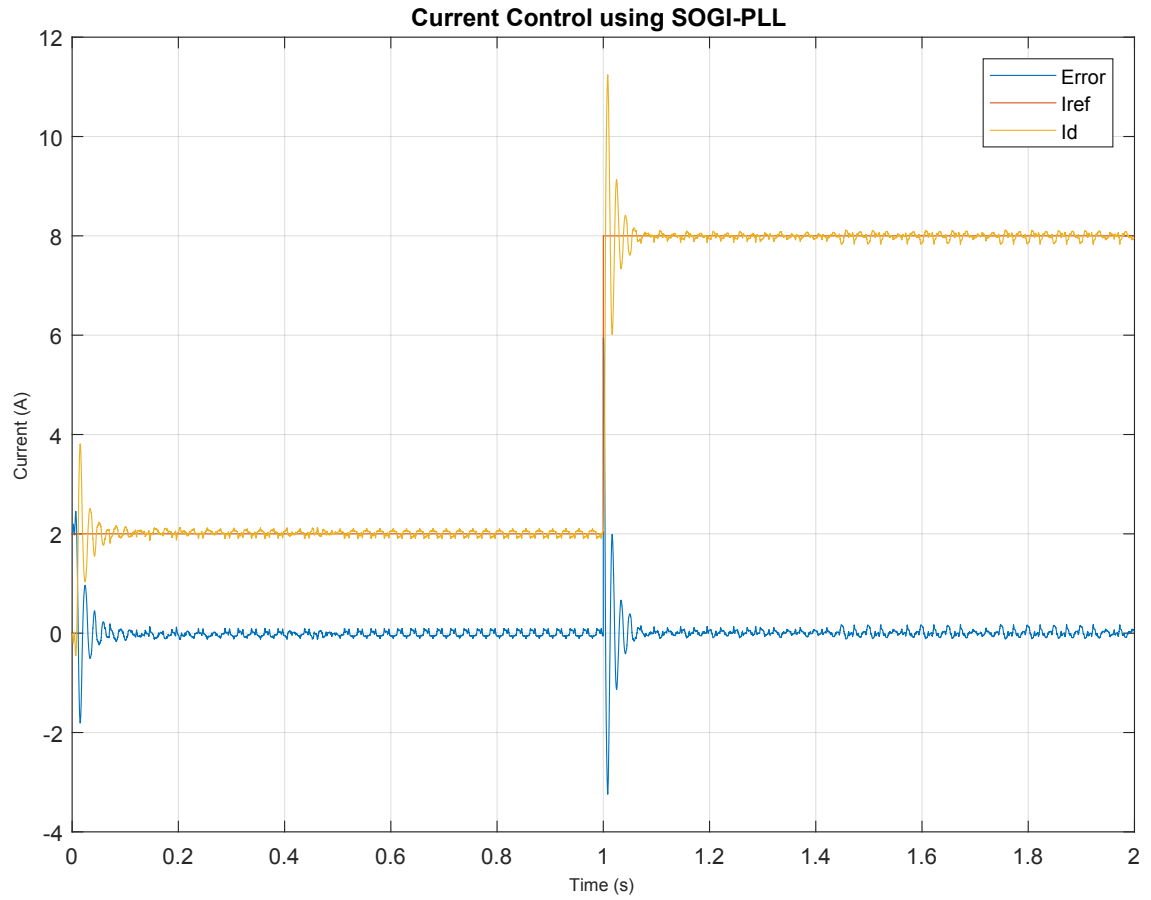


Figure 3.7: VOC SOGI based PLL.

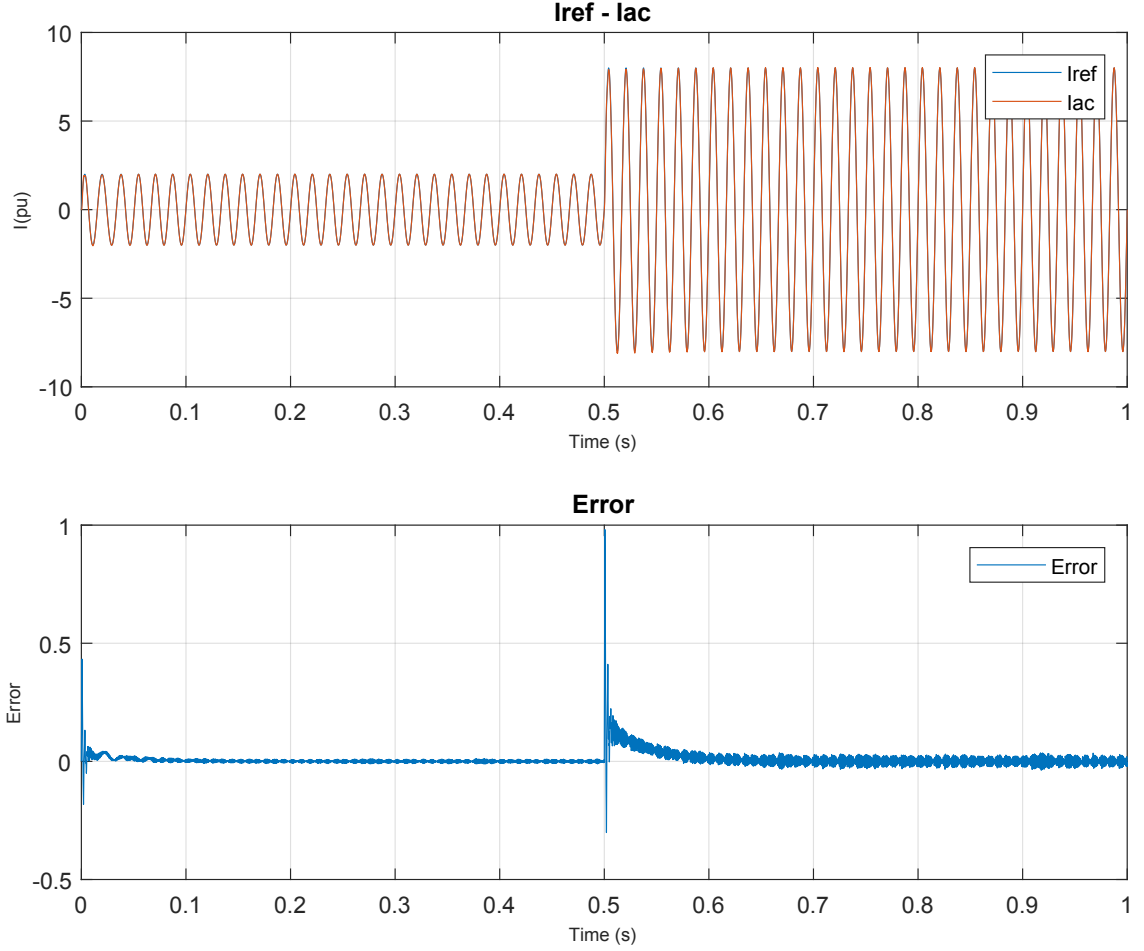


Figure 3.8: PR SOGI based PLL.

3.4 Summary of the chapter

This chapter discussed two classical control approaches for single phase converters, voltage oriented control (VOC) and proportional resonant (PR). To analyze in detail each control goes beyond the scope of this thesis. Nevertheless, the methods were presented in general to get a basic idea of the concept. Additionally they were implemented in SIMULINK/MATLAB software and its results were shown in the previous section.

From the results we can conclude that the PR shows a much more straightforward model, specially for single phase systems, which is the concern of this thesis. Thus, this approach does not require axis transformations, therefore its implementation is simpler as well. Hence, this technique will be used for further analysis in this work.

However, notice that although the control is based in a frequency domain analysis, its implementation is non linear. Therefore we require a non linear analysis in order to consider the dynamics in any rigorous analysis. Next chapter will develop a non linear stability analysis based on Lyapunov theory.

Chapter 4

Stability analysis

Proportional resonant control is well known method for single phase VSC, its objective is to track sinusoidal references, thus, for this particular case it will not require any axis transformation, this is due to its measured signals are already in $\alpha\beta$, since the a, b, c frame is the same stationary frame for single phase systems.

Voltage oriented control requires dq transformation and it has proven a good performance for three phase or balanced systems, but this is not the case. As mentioned before, to apply such concept it has to be adapted for single phase applications. One solution to this, is to design a fictitious axis and perform the synchronous reference frame transformation. However, this is an extra step which adds computational effort and therefore delay.

These types of controllers are designed to protect the conversion system from high currents, that is one reason why they are build in layers and the first one is the current control. So they are not oriented to analyze which conditions are prone to instability problems. Therefore, study the stability of the classical and well known control techniques can provide valuable information, e.g. the limits of the control parameters, especially to understand the stability boundaries of the system.

It is important to keep in mind that ac conversion systems are complex and highly non linear, this is mainly due to the switching devices. Hence, applying a control technique which can be described in time domain along with the system model would generate a complete model of the system in the same reference frame. That is the case of P-R control, which allows to represent its model in time domain, since we are avoiding axis transformation.

Furthermore, the stability analysis for such complex and non linear systems can be either frequency or time domain methods. Among the frequency methods the most popular is the small signal impedance-based stability criterion, which applies the Nyquist criterion, this is a very useful analysis to establish stability boundaries, however this is still a linearized method. For time domain methods the most common approach is based on eigenvalues analysis, which is also small signal analysis, a linearized approach as well.

Notice that the single phase VSC based on P-R control describes a non linear model in time domain, therefore, in order to keep the dynamics of the mentioned system and to establish some limits for the controller parameters, a non linear stability analysis can be suitable for such system.

Moreover, it is worth notice that the PLL is assumed to be adequately tuned and its performance will allow it to synchronize properly to the grid. This assumption is required in order to apply the “*vanishing perturbation theorem*” from Lyapunov theory [40], explained later in this chapter.

Along this chapter a non linear stability analysis will be described for the single phase VSC based on the proportional resonant PR-controller, this with the aim of proving, based on the stability analysis, how should be the properties of the controller parameters. It is important to establish some limits to define these parameters, specially to ensure stability of a well known method.

The model of the proportional resonant control is usually expressed by a transfer function, but this is easily converted to the time domain, as follows:

The transfer function of the proportional-resonant control (3.7) is equivalent to the following state-space representation, as mentioned in the previous Chapter.

$$\begin{pmatrix} \dot{z}_1 \\ \dot{z}_2 \end{pmatrix} = \begin{pmatrix} 0 & 1 \\ -\omega^2 & 0 \end{pmatrix} \begin{pmatrix} z_1 \\ z_2 \end{pmatrix} + \begin{pmatrix} k_i \\ 0 \end{pmatrix} u$$

$$y = z_1 + k_p u$$

In this case, u comes from the dc-side control and is given by

$$u = I_{ref} f_{PLL}(\omega t) - i_{ac}$$

where $f_{PLL}(\omega t)$ represents the input from the phase-locked-loop (PLL) and i_k is the ac current with the direction shown in Fig 3.3. In these equations ω is the frequency estimated

by the PLL which is equal to the stationary state frequency of the grid if the PLL is properly designed. The dynamics of the output filter (or ac side) is also represented as follows

$$y = L \frac{di_{ac}}{dt} + Ri_{ac} + V_s$$

this is similar to Equation 3.1. Let us analyze the stability of the proportional-resonant current control for a single-phase inverter which dynamics are given as follows:

$$\begin{aligned} \frac{d}{dt} \begin{pmatrix} i_{ac} \\ z_1 \\ z_2 \end{pmatrix} &= \begin{pmatrix} \frac{-R_s - k_p}{L_s} & \frac{1}{L_s} & 0 \\ -k_i & 0 & 1 \\ 0 & -\omega^2 & 0 \end{pmatrix} \begin{pmatrix} i_{ac} \\ z_1 \\ z_2 \end{pmatrix} \\ &+ \begin{pmatrix} \frac{1}{L_s} \\ 0 \\ 0 \end{pmatrix} f(t) + \begin{pmatrix} \frac{k_p I_{ref}}{L_s} \\ k_i I_{ref} \\ 0 \end{pmatrix} f_{PLL}(\omega t) \end{aligned} \quad (4.1)$$

where $v_s = v_m f(t)$ and $f_{PLL} = f(t)$ if the PLL works correctly. Notice that this system is non-autonomous. The stability of the system is given by (4.1) depends on the properties of the matrix A defined as follows

$$A = \begin{pmatrix} \frac{-R_s - k_p}{L_s} & \frac{1}{L_s} & 0 \\ -k_i & 0 & 1 \\ 0 & -\omega^2 & 0 \end{pmatrix}$$

let us calculate the principal minors

$$D_{A(1)} = -\frac{R_s}{L_s} - \frac{k_p}{L_s} < 0 \quad (4.2)$$

$$D_{A(2)} = \det \begin{pmatrix} -\frac{R_s}{L_s} - \frac{k_p}{L_s} & 1 \\ -k_i & 0 \end{pmatrix} = k_i > 0 \quad (4.3)$$

$$D_{A(3)} = \det(A) = -\omega^2 \left(\frac{R_s}{L_s} + \frac{k_p}{L_s} \right) < 0 \quad (4.4)$$

since $D_{A(i)}$ alternates in sign then A is negative definite and hence the dynamical system is asymptotically and exponentially stable.

In steady state, we have the following:

$$\dot{X}_s = (A_0 + \omega^2 A_1) X_s + \underbrace{b_1 f(t)}_{V_s} + \underbrace{b_2 f(t)}_{I_{ref PLL} = i_{ac}} \quad (4.5)$$

$$A = A_0 + \omega^2 A_1 \quad (4.6)$$

for the model, $f(t)$ comes out from the PLL, it can be considered as a time variant external disturbance.

Using the following variable change:

$$y = x - x_s$$

$$\dot{y} = \dot{x} - \dot{x}_s$$

$$\dot{y} = (A_0 + \omega^2 A_1) x + b_2 f_{PLL}(t) - A_0 x_s - \omega_0^2 A_1 x_s - b_2 f_{PLLss}(t)$$

$$\dot{y} = (A_0 + \omega^2 A_1) y + \overbrace{A_1 x_s (\omega^2 - \omega_0^2) + b_2 (f_{PLL}(t) - f_{PLLss}(t))}^{g(t)}$$

$$\dot{y} = \underbrace{(A_0 + \omega^2 A_1)}_{<0} y + \underbrace{g(t)}_{\text{vanishing Disturbance}}$$

A Lyapunov function is proposed:

$$V = y^T P y \quad (4.7)$$

Where P is a constant and symmetric matrix, and its derivative is given by equation 4.9

$$\dot{V}(t, y) = \dot{y}^T P y + y^T P \dot{y} \quad (4.8)$$

$$\begin{aligned} \dot{V}(t, y) &= \left[y^T (A_0 + \omega^2 A_1)^T + x_s^T A_1^T (\omega^2 - \omega_0^2) + (f_{PLL}(t) - f_{PLLss}(t)) b_2^T \right] P y \\ &\quad + y^T P \left[(A_0 + \omega^2 A_1) y + A_1 x_s (\omega^2 - \omega_0^2) + (f_{PLL}(t) - f_{PLLss}(t)) b_2 \right] \\ \dot{V}(t, y) &= [y^T A^T + g(t)] P y + y^T P [A y + g(t)] \\ \dot{V}(t, y) &= \underline{y^T A^T P y} + g(t) P y + \underline{y^T P A y} + y^T P g(t) = y^T \underbrace{(A^T P + P A)}_{-Q} y + \frac{\partial V}{\partial y} g(t) \end{aligned}$$

$$\dot{V}(t, y) = -y^T Q y + \underbrace{g(t) P y + y^T P g(t)}_{2y^T P g(t)} = -y^T Q y + 2y^T P g(t) \quad (4.9)$$

Using the theory of vanishing perturbation from [40] which states that a Lyapunov function $V : D \rightarrow \mathfrak{R}$ is exponentially stable if satisfies the following conditions:

$$c_1 \|y\|^2 \leq V(t, y) \leq c_2 \|y\|^2 \quad (4.10)$$

$$\frac{\partial V}{\partial t} + \frac{\partial V}{\partial y} f(t, x) \leq -c_3 \|y\|^2 \quad (4.11)$$

$$\left\| \frac{\partial V}{\partial y} \right\| \leq c_4 \|y\| \quad (4.12)$$

for all $(y, t) \in [0, \infty) \times D$ for some positive constants c_1, c_2, c_3 and c_4 . Where the perturbation term $g(t, y)$ satisfies the linear growth bound

$$\|g(t, y)\| \leq \gamma \|y\|, \forall t \geq 0, \forall y \in D \quad (4.13)$$

where γ is a non negative constant.

Following the vanishing perturbation theory we have:

$$c_1 \|y\|^2 \leq V(t, y) \leq c_2 \|y\|^2 \quad c_1 < \|P\|, \quad c_2 > \|P\| \quad (4.14)$$

$$\dot{V}(t, y) = \underbrace{\frac{\partial V}{\partial t} + \frac{\partial V}{\partial y} f(t, y)}_{\leq -c_3 \|y\|^2} + \frac{\partial V}{\partial y} g(t, y) \quad (4.15)$$

$$\dot{V}(t, y) \leq -c_3 \|y\|^2 + \left\| \frac{\partial V}{\partial y} \right\| \|g(t, y)\| \quad (4.16)$$

$$\dot{V}(t, y) \leq -c_3 \|y\|^2 + c_4 \|\gamma\| \|y\|^2 \quad (4.17)$$

$$\dot{V}(t, y) = -y^T Q y + 2y^T P g(t) \leq -c_3 \|y\|^2 + c_4 \|\gamma\| \|y\|^2 \quad (4.18)$$

$$c_4 = \|2P\| \quad (4.19)$$

$$\|\gamma\| < \frac{c_3}{c_4} \quad (4.20)$$

$$c_3 \geq \|Q\| \quad (4.21)$$

Remember that $-Q = A^T P + P A$, with $P = Identity$ and $\|Q\|$ can be the euclidean norm or any norm. For example, the infinity norm, which is given by $\|Q\|_\infty = \max \sum |a_{ji}|$. Hence, the matrix Q is:

$$-Q = \begin{pmatrix} \frac{-2k_p - 2R_s}{L} & \frac{1}{L} - k_i & 0 \\ \frac{1}{L} - k_i & 0 & 1 - \omega^2 \\ 0 & 1 - \omega^2 & 0 \end{pmatrix} \quad (4.22)$$

$$\|Q\| = \max \left[\left| \frac{2k_p + 2R_s}{L} \right| + \left| k_i - \frac{1}{L} \right|, \left| k_i - \frac{1}{L} \right| + |\omega^2 - 1|, |\omega^2 - 1| \right] \quad (4.23)$$

From Equation 4.4 the lower limits of the controller parameters were established, this means, $k_p > -R_s$ $k_i > 0$. Which will be needed in the following analysis:

If we assume that $\omega = \omega_{pu} = 1$, then $\|Q\|$ will be in terms of the control parameters:

$$\left| \frac{2k_p + 2R_s}{L} \right| + \left| k_i - \frac{1}{L} \right| < c_3 \quad (4.24)$$

$$\left| k_i - \frac{1}{L} \right| + \underbrace{|\omega_{pu}^2 - 1|}_0 < c_3 \quad (4.25)$$

therefore:

$$\|Q\| = \left| \frac{2k_p + 2R_s}{L} \right| + \left| k_i - \frac{1}{L} \right| < c_3 \quad (4.26)$$

from which the mentioned limits for the controller parameters can be established in terms of the circuit parameters and the constant c_3 .

$$0 < k_i < c_3 + \frac{1}{L} \quad (4.27)$$

$$-R_s < k_p < \frac{L}{2}c_3 - R_s \quad (4.28)$$

In order to determine the constants c_3 and c_4 as mentioned in Equation 4.12, we can start from remembering that Equation 4.13: $\|g(t, y)\| \leq \gamma \|y\|$ can express any norm. And if we consider the second norm, then γ can be a quadratic error. Also, if P is the identity matrix, then $c_4 = 2$, as mentioned in Equation 4.19. Hence, we can find a value for c_3 in terms of the quadratic error and the constant c_4 :

$$\gamma \cdot c_4 = c_3 \quad (4.29)$$

And finally the controller parameters (k_p , k_i) can be defined in between the limits described above, which can guarantee, by Lyapunov theory, the stabilization of the system.

4.1 Results

This section is dedicated to prove the Lyapunov theory mentioned along this Chapter. So, in order to validate the previous analysis, several cases were tested by varying the controller parameters k_p and k_i , also the phase deviation was considered in the performed tests.

For simplicity and with the aim of showing the complete results of some of the evaluated scenarios, in this Section three different cases will be shown, two unstable cases and one stable case. For the first case, the controller parameters were chosen to be $k_p = 0.06$ and $k_i = 0.6$, this result is depicted in Fig. 4.1, the second is in Fig. 4.2, from which $k_p = 0.03$ and $k_i = 3.4$. Both cases were unstable operational points, it can be observed from these results that no matter if the controller starts tracking with good performance the reference signal, it may be unstable later on, this is visible in Fig. 4.1. Thus, some values of the parameters can always cause an unstable scenario, that is the case of Fig. 4.2, in which the controller is lost from the very beginning.

As mentioned before, all the tested cases considered a small variation of the frequency in the system (in the acceptable range of deviation “Dead-band”), this is not a such a critical problem for the controller, since the SOGI-PLL is working on this issue.

Moreover all the tested cases produced an error from which we can conclude that there exist a region in which the values of the controller parameters can lead to a stable control operation, this is depicted in Fig. 4.4, from which, the yellow points enclose the stable region and the blue points portray the unstable region. Thus, each point is a combination of the values of the parameters, such combination is represented in the axis of the mentioned figure. For every evaluated point an error signal is generated and analyzed to develop an algorithm and be able to study several cases and compare them.

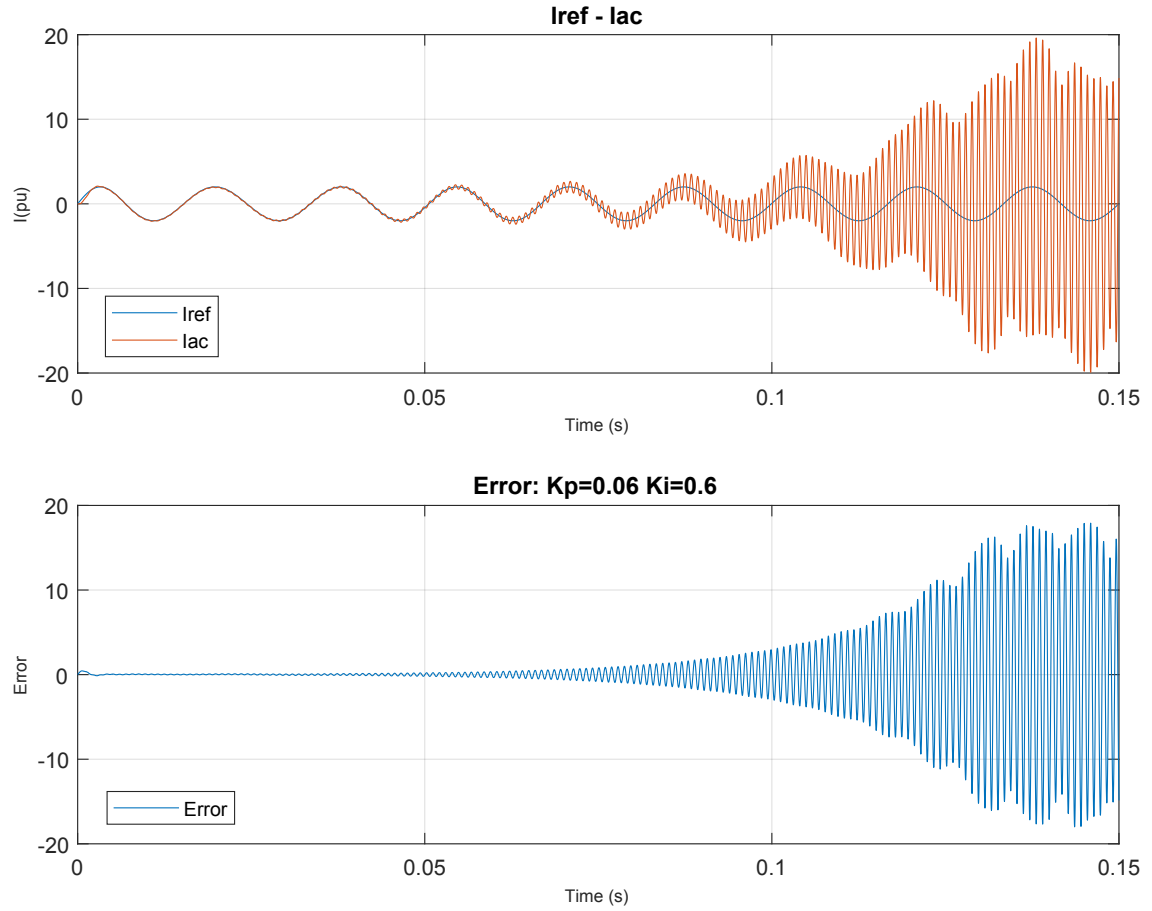


Figure 4.1: PR-SOGI study case SIMULINK/MATLAB based, with $K_p = 0.06$ $K_i = 0.6$.

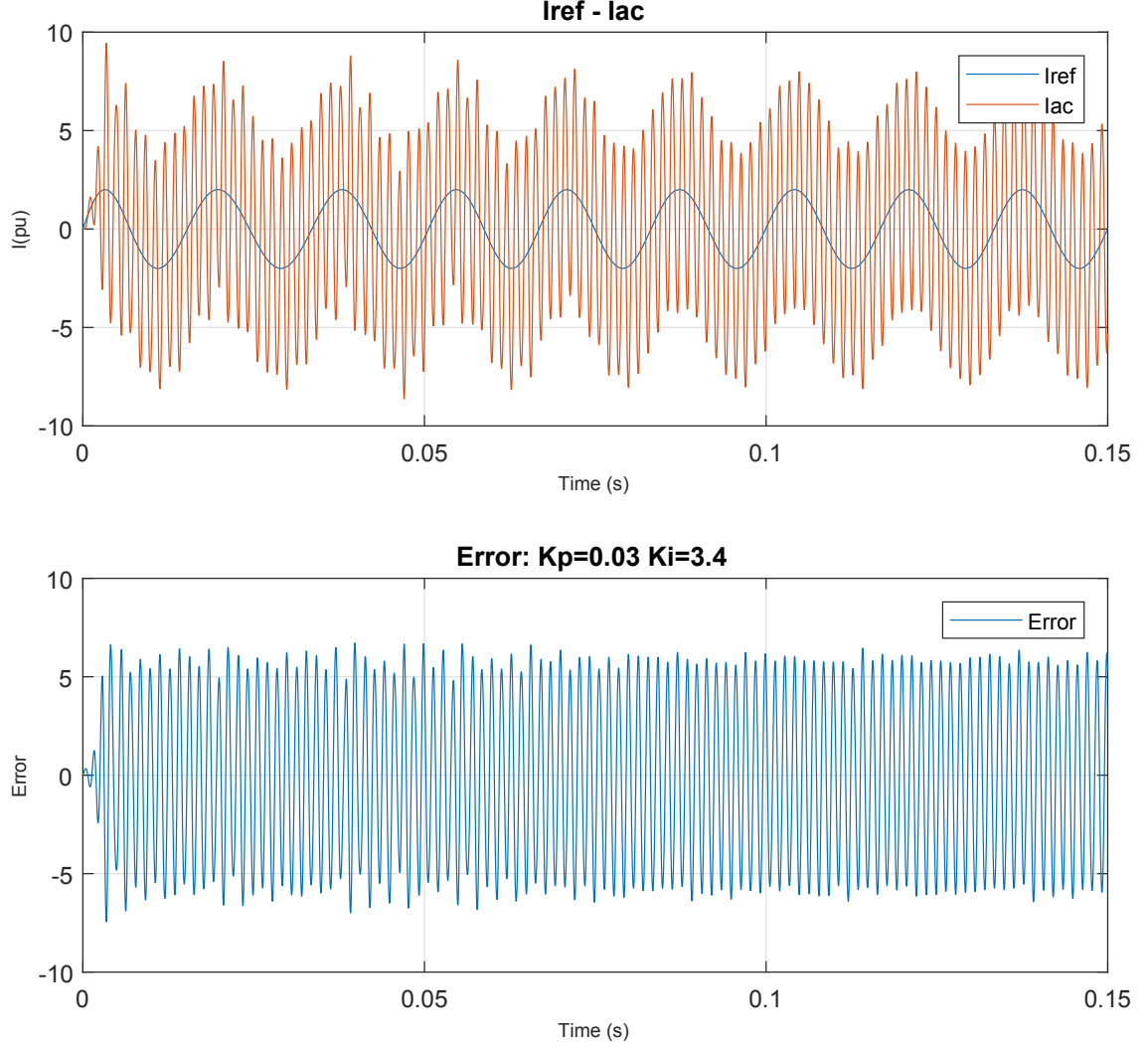


Figure 4.2: PR-SOGI study case SIMULINK/MATLAB based, with $K_p = 0.03$ $K_i = 3.4$.

The third case, on the contrary, represents a stable scenario, in which the controller parameters are designed to be: $k_p = 0.04$ and $k_i = 1.3$. The response of this scenario is shown in Fig. 4.3. From here it can be observed that, this combination of parameters allows the controller to follow accurately the reference signal, there is a noticeable difference with the other two scenarios shown before.

Notice that this is not the unique stable point, as mentioned before, several test on this controller were considered by changing the parameters k_p and k_i . Fig. 4.4 shows the relationship between the controller parameters. After evaluating any selected values of the parameters, the mean squared error (MSE) is calculated from the error signal, procedure executed for each scenario. This with the purpose of establishing an algorithm to state which system represent an unstable or stable operational point. For this particular case, the MSE was considered to be small enough for the stable scenarios. In Fig.4.4 a stable region is formed by the yellow points and an unstable region by the dark blue points. From here we can say that K_i can not go further from the value 2.5 and k_p from 0.06.

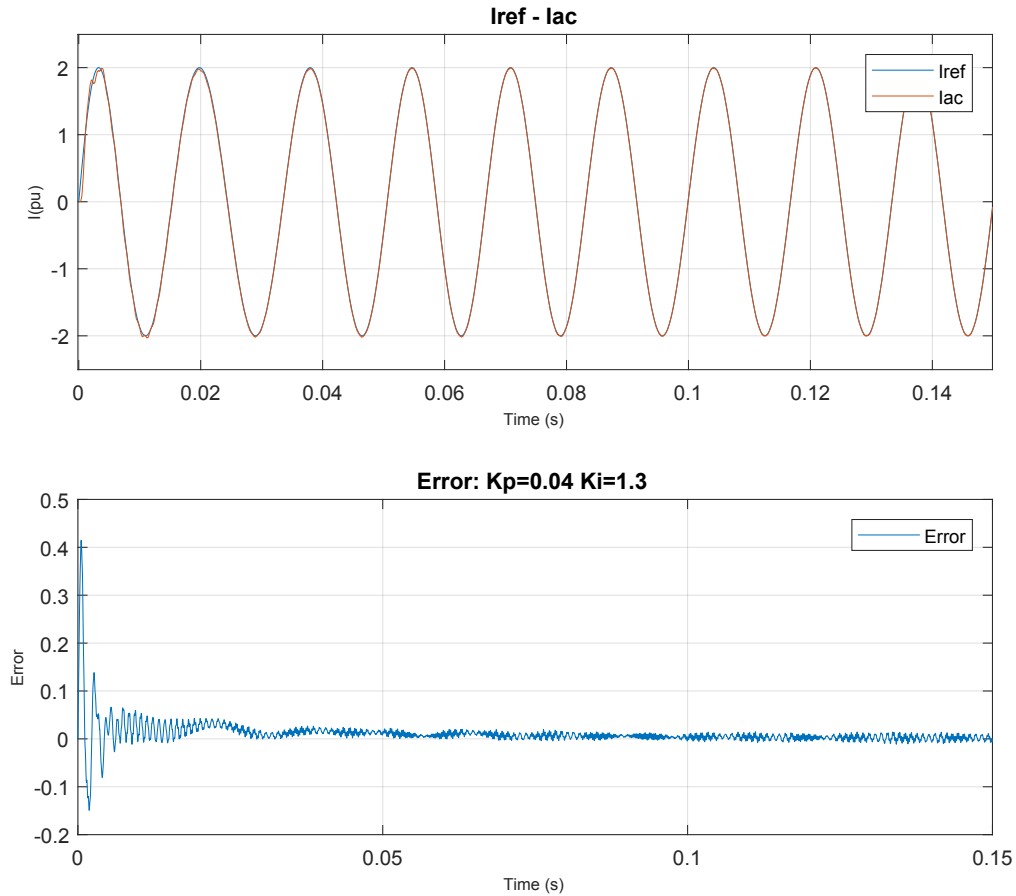


Figure 4.3: PR-SOGI study case SIMULINK/MATLAB based, with $k_p = 0.04$ $k_i = 1.3$.

It is important to remember that, from Equation 4.2 we got a limit for k_p , which states

that $k_p > -R_s$, thus a limit for $k_i > 0$. This can be verified in Fig.4.4, where k_p can not be lower than $-R_s$, for this particular case $R_s = 0.015\Omega$ and this is accomplished and visible. If this conditions are not fulfilled, the system will be unstable, as stated in the stability analysis by the principal minors. Thus, this limits were stated before applying the vanishing perturbation theory.

Furthermore, the mentioned study cases are highlighted in Fig.4.4, from which it can be notice that the unstable scenarios are within the blue region, in the same way the stable case is into the yellow region, which represents the stable region for a combination of values in the controller parameters.

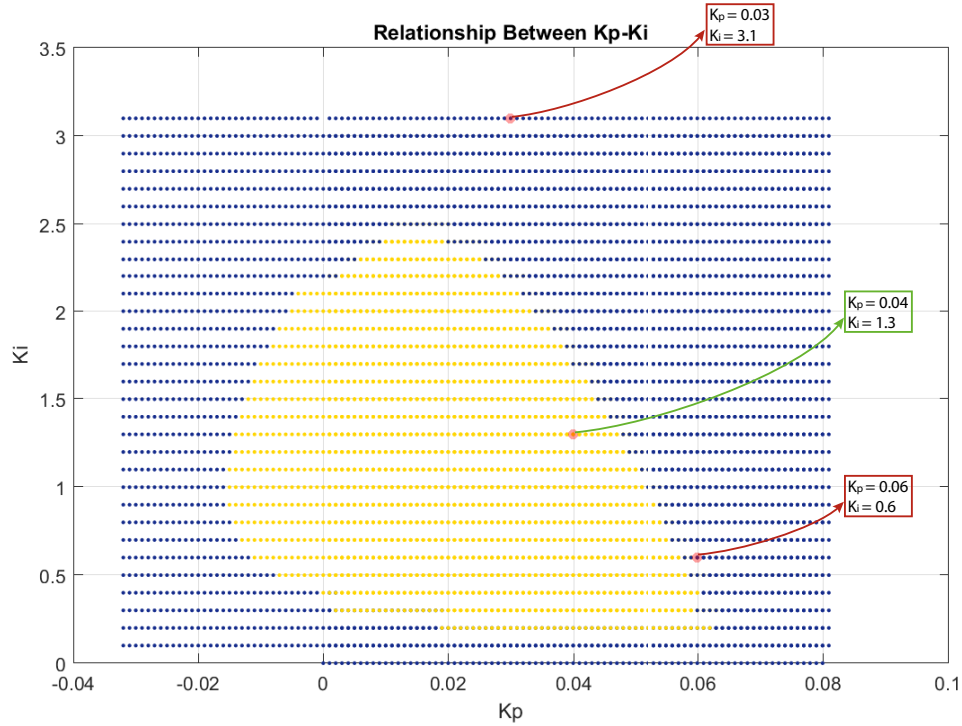


Figure 4.4: Relation between k_i - k_p in the PR-SOGI study case SIMULINK/MATLAB based. The yellow points are related to stable operational states and the blue points represent unstable states.

4.2 Summary of the Chapter

Through this Chapter a stability analysis is described with the purpose to establish a mathematical representation of the classical proportional resonant control for single phase power converters and analyze the stability properties of such system.

The stability analysis was performed based on the vanishing perturbation theorem from Lyapunov Theory, this with the purpose of establishing the conditions for the controller to operate properly. From here we could conclude, from the principal minors definition, that the parameters of the proportional resonant control had to fulfill the following conditions: $k_p > -R_s$ and $k_i > 0$.

Several cases were tested in order to compare the simulation with the described mathematical procedure. An algorithm to vary the controller parameters was designed and from each combination the mean squared error (MSE) between the reference and the control signal was calculated. As a result, all the tested cases were compared by the MSE and its result is shown in Fig. 4.4, in which the yellow points represent the MSE lower than 0.01, this means that the control was working properly and following the reference signal. Therefore, this yellow region establish the cases where the stability is ensured.

On the other hand, the blue points represent the cases where the MSE was showing that the performance of the control technique was not able to follow the reference signal, and therefore this depicts the unstable region. Thereby the implemented results validate the proposed stability analysis, by the established limits of the controller parameters.

Conclusions

This chapter recapitulates the main results of this thesis and presents some recommendations for further investigations.

- The synchronization issue is studied, particularly for single phase converters, four different types of orthogonal signal generators were studied and compared. Derivative, integral, delay and second order generalized integrator. As a conclusion we can say that the SOGI-PLL presented a better performance, since we compare both, the quadrature generated signal and the detected frequency. From these results the SOGI-PLL manage to overcome the frequency step at 0.56s and stabilize it self quickly, but the others did not manage to properly follow the reference signal after the step change.
- Two classical control techniques were studied and also compared, the vector control based on the synchronous reference frame and the proportional resonant control based on the stationary reference frame. This with the purpose of understanding the models which can describe them, thus, in order to analyze its stability properties. The P-R control model can be analyzed by Lyapunov theory, this is mainly due to its implementation directly in *abc* frame, so the reference frame transformations are avoided.
- The single phase VSC based on P-R control describes a non linear model in time domain, therefore, in order to keep the dynamics of the mentioned system and to establish some limits for the controller parameters, a non linear stability analysis is accomplished, based on the assumption that the PLL will manage to perform properly so the error in steady state will tend to zero, then it could be seen as a vanishing perturbation. The results show a stable region to select the values of the controller parameters k_p and k_i . This is achieved by Lyapunov theory and simulation analysis (SIMULINK/MATLAB). From here we can conclude that the implemented results confirm the proposed analysis.

Future research work

- Appendix A, will describe a proposal for further investigation, this is focused on the development of a control technique for single phase VSC considering within its design the synchronization, this means without the classical PLL or any other type of element apart from the same controller. The idea is mathematically developed in terms of stability analysis by Lyapunov theory. However, it is not completely finished, since it has no implemented results so far.

Appendix A

Lyapunov based control for SPVSC

In this Appendix a different approach for controlling the single phase VSC is proposed, in which the synchronization is included within its design, thus, the dynamics of the system are considered through the differential equations that model mathematically such system.

One of the reasons why classical control techniques develop it success quickly is because they are usually build up in layers, the synchronization layer, the current control layer, the voltage and power control layer. In this approach, the control techique will consider all the stages in one control loop.

The mathematical description and demonstration of the designed control based on stability analysis is shown in the following pages.

We can start from remembering Equation 3.1, which is the same as the Equation A.1, this one describes the circuit on the ac side, and it is quite a general expression.

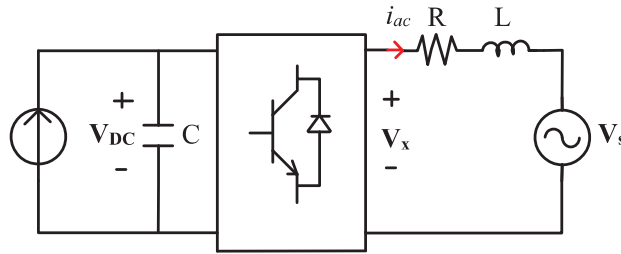


Figure A.1: Single phase VSC

$$mV_{DC} = Ri_{ac} + L \frac{di_{ac}}{dt} + V_s(t) \quad (\text{A.1})$$

Where $V_s(t)$ is the grid voltage of the form $V_s = A \cdot \cos(\omega t + \phi)$, which is T- periodic. Notice that the time is explicitly in the equation. Therefore the system is time dependent.

$$\frac{P}{V_{DC}} = C \frac{dV_{DC}}{dt} + I_{DC} \quad (\text{A.2})$$

It is assumed that the switching frequency is high and also the converter is a lossless system.

$$P_{ac} = P_{DC}$$

$$V_x i_{ac} = V_{DC} I_{DC}$$

average model:

$$mV_{DC} = V_x$$

$$I_{DC} = \frac{V_x i_{ac}}{V_{DC}} = m i_{ac} \quad (\text{A.3})$$

Equation A.2 becomes

$$P = \frac{C}{2} \frac{dV_{DC}^2}{dt} + mV_{DC} i_{ac} \quad (\text{A.4})$$

The state variables are define as follows:

$$x_1 = i_{ac} - kVs(t) \quad (\text{A.5})$$

Where x_1 is the error for the current controller, since the desired current will be in phase with the grid voltage, meaning that i_{ac} will be proportional to $V_s(t)$.

$$x_2 = V_{DC}^2 - V_{DCref}^2 \quad (\text{A.6})$$

The control is divided in two dynamics, one slow and the other accelerated:

$$u + \tilde{u} = mV_{DC} \quad (\text{A.7})$$

Where u will depend only of the states variables $u = u(x_1, x_2)$ and \tilde{u} will depend on time $\tilde{u} = u(t)$.

Hence, the model is:

$$u + \tilde{u} = R(x_1 + kV_s(t)) + L \frac{d}{dt}(x_1 + kV_s(t)) + V_s(t)$$

$$u + \tilde{u} = Rx_1 + RkV_s(t) + L\dot{x}_1 - Lk \frac{dV_s(t)}{dt} + V_s$$

$$\tilde{u} = RkV_s + V_s - Lk \frac{dV_s}{dt}$$

$$u = Rx_1 + L\dot{x}_1$$

Equation A.2 is rewritten as:

$$P = \frac{C}{2}\dot{x}_2 + (u + \tilde{u})(x_1 + kV_s)$$

$$P = \frac{C}{2}\dot{x}_2 + ux_1 + ukV_s + \tilde{u}x_1 + \tilde{u}kV_s$$

A.1 Averaging

With a scaling of the time as $T = \omega t$, \dot{x}_2 becomes $\dot{x}_2 \rightarrow \omega \dot{x}_2$

$$\omega \dot{x}_2 = \frac{2}{C} (P - ux_1 - ukV_s - \tilde{u}x_1 - \tilde{u}kV_s) \quad (\text{A.8})$$

Let $\varepsilon = \frac{1}{\omega}$ which is a small value ($\frac{1}{2*\pi*f}$). Then if the dynamics from the DC side is slow, the averaging method is applied:

$$\begin{aligned} \dot{x} &= \varepsilon f(x, t) \\ \dot{\bar{x}} &= \bar{f}(\bar{x}) \\ \bar{f} &= \int_t^{t+T} f(\bar{x}, t) \end{aligned}$$

$$\dot{\bar{x}}_1 = \frac{1}{L} (-R\bar{x}_1 + \bar{u}) \quad (\text{A.9})$$

$$\dot{x}_2 = \frac{2}{C\omega} (P - ux_1 - ukV_s - \tilde{u}x_1 - \tilde{u}kV_s) \quad (\text{A.10})$$

$$\begin{aligned} \dot{x}_2 &= \frac{2}{C} \left(\int_t^{t+T} [P - ux_1 - ukV_s - \tilde{u}x_1 - \tilde{u}kV_s] dt \right) \\ \dot{x}_2 &= \frac{2}{C} \left(\bar{P} - \bar{u} \cdot \bar{x}_1 - \underbrace{\int_0^T ukV_s}_{\alpha} - \bar{x}_1 \underbrace{\int_0^T \tilde{u}}_{\alpha} - \underbrace{\int_0^T \tilde{u}kV_s}_{\phi} \right) \end{aligned}$$

Where $\alpha = 0$ since the average value of a sinusoidal signal is zero, as follows:

$$\begin{aligned} \alpha &= \int_0^T \tilde{u} = \int_0^T \left(RkV_s + V_s - Lk \frac{dV_s}{dt} \right) dt \\ \alpha &= Rk \int_0^T A \cos(\omega t + \phi) dt + \int_0^T A \cos(\omega t + \phi) dt - Lk \int_0^T \frac{d}{dt} (A \cos(\omega t + \phi)) dt = 0 \\ \dot{x}_2 &= \frac{2}{C} \left(\bar{P} - \bar{u} \cdot \bar{x}_1 - \underbrace{\int_0^T \tilde{u}kV_s}_{\phi} \right) \end{aligned} \quad (\text{A.11})$$

If k is designed in such way that:

$$\bar{P} = \phi = \frac{1}{T} \int_0^T \tilde{u}kV_s \quad (\text{A.12})$$

Then the system equations in average mode will be:

$$\dot{\bar{x}}_1 = \frac{1}{L} (-R\bar{x}_1 + \bar{u}) \quad (\text{A.13})$$

$$\dot{\bar{x}}_2 = \frac{2}{C} (-\bar{u} \cdot \bar{x}_1) \quad (\text{A.14})$$

Using Input-to-State Stability analysis (ISS) [40].

- If a system is ISS then:

- (a) for $u \equiv 0$ the origin is globally asymptotically stable (GAS).
- (b) for a bounded input u , every solution $x(t)$ is bounded.

if $u = 0$:

$$\dot{x}_1 = -\frac{R}{L}x_1$$

$$\dot{x}_2 = 0$$

The Lyapunov function candidate for this case is:

$$V_1 = \frac{1}{2} (x_1^2 + x_2^2) \quad \text{is} \quad \begin{cases} C^1 & \text{continuosly differentiable} \\ V_1 > 0 & \text{possitive definite} \\ V_1(0,0) = 0 \\ V_1 \leq \Omega_c & \text{is bounded} \end{cases}$$

$$\dot{V}_1 = -\frac{R}{L}x_1^2 \leq 0 \quad \text{possitive semidefinite} \quad (\text{A.15})$$

Since \dot{V}_1 is possitive semidefinite ($\dot{V}_1(0, x_2) = 0$), and V_1 fulfill the conditions to apply LaSalle method, this will be the next step.

$$\text{Let } E = \left\{ x \in \mathbb{R}^2 \mid \dot{V}(x) = 0 \right\} \quad (\text{A.16})$$

$$\dot{V}(x) = 0 \quad = -\frac{R}{L}x_1^2 \rightarrow x_1 = 0 \quad (\text{A.17})$$

$$M : (x_1, x_2) \in M \subset E \rightarrow x_1 = 0 \rightarrow \dot{x}_2 = 0 \rightarrow \textcolor{red}{x}_2 = 0 \quad (\text{A.18})$$

if A.18 is true, then $M = (0, 0)$ and it would be GAS!.

In any case for the complete equation system A.13 and A.14 the Lyapunov function candidate is chosen as a quadratic function:

$$V_2 = \frac{1}{2} (x_1^2 + x_2^2) \quad \text{is} \quad \begin{cases} C^1 & \text{continuosly differentiable} \\ V_2 > 0 & \text{possitive definite} \\ V_2(0, 0) = 0 \\ V_2 \leq \Omega_c & \text{is bounded} \end{cases}$$

Where its derivative is:

$$\dot{V}_2 = -\frac{R}{L}x_1^2 + \frac{1}{L}ux_1 - \frac{2}{C}ux_1x_2 \quad (\text{A.19})$$

$$\dot{V}_2 = -\frac{R}{L}x_1^2 + ux_1 \left(\frac{1}{L} - \frac{2}{C}x_2 \right) \quad (\text{A.20})$$

Designing u such that the derivative is negative definite $\dot{V}_2 < 0$:

$$u = -x_1(1 - x_2) \quad (\text{A.21})$$

replacing u into equation A.20

$$\dot{V}_2 = -\frac{R}{L}x_1^2 - (x_1(1-x_2))x_1 \left(\frac{1}{L} - \frac{2}{C}x_2 \right)$$

$$\dot{V}_2 = -\frac{R}{L}x_1^2 - x_1^2 \left(\frac{1}{L} - \frac{1}{L}x_2 - \frac{2}{C}x_2 + x_2^2 \right)$$

$$\dot{V}_2 = -\frac{R}{L}x_1^2 - x_1^2 \left(\frac{1}{L} + \underbrace{x_2^2 - \left(\frac{1}{L} + \frac{2}{C} \right) x_2}_{\leq 0} \right)$$

$$x_2^2 - \left(\frac{1}{L} + \frac{2}{C} \right) x_2 \leq 0 \quad \rightarrow \quad x_2 \leq \left(\frac{1}{L} + \frac{2}{C} \right)$$

$$\dot{V}_2 = -\frac{R}{L}x_1^2 - x_1^2 \left(\frac{1}{L} + x_2^2 \right) \quad \rightarrow \quad \dot{V}_2 \leq 0$$

With the system from equations A.13, A.14 and A.21, the new system is:

$$\dot{\bar{x}}_1 = \frac{1}{L} (-R\bar{x}_1 - \bar{x}_1 + \bar{x}_1\bar{x}_2) \tag{A.22}$$

$$\dot{\bar{x}}_2 = -\frac{2}{C}\bar{x}_1^2(1-\bar{x}_2) \tag{A.23}$$

which is globally asymptotically stable (GAS) based on Lyapunov theory.

It is important to remember from equation A.12, that the following condition must be fulfilled:

$$P = \phi = \frac{1}{T} \int_0^T \left(RkV_s + V_s - Lk \frac{dV_s}{dt} \right) kV_s dt \tag{A.24}$$

$$\phi = \frac{1}{T} \int_0^T (Rk^2V_s^2) dt + \frac{1}{T} \int_0^T (kV_s^2) dt - \frac{1}{T} \int_0^T \left(Lk^2V_s \frac{dV_s}{dt} \right) dt \tag{A.25}$$

$$\phi = Rk^2 \underbrace{\frac{1}{T} \int_0^T (V_s^2) dt}_a + k \underbrace{\frac{1}{T} \int_0^T (V_s^2) dt}_a - Lk^2 \underbrace{\frac{1}{T} \int_0^T \left(V_s \frac{dV_s}{dt} \right) dt}_b \quad (\text{A.26})$$

Where a and b are known parameters from the measured voltage grid V_s .

$$P - (Ra - Lb) k^2 - ak = 0 \quad (\text{A.27})$$

Bibliography

- [1] P. Sreekumar, R. Danthakani, and S. P. Veettil, "Implementation of proportional-resonant controller in an autonomous distributed generation unit," in *2018 Advances in Science and Engineering Technology International Conferences (ASET)*, Feb 2018, pp. 1–5.
- [2] S. Deo, C. Jain, and B. Singh, "A pll-less scheme for single-phase grid interfaced load compensating solar pv generation system," *IEEE Transactions on Industrial Informatics*, vol. 11, no. 3, pp. 692–699, June 2015.
- [3] D. Del Puerto-Flores, J. M. A. Scherpen, M. Liserre, M. M. J. De Vries, M. J. Kransse, and V. G. Monopoli, "Passivity-based control by series/parallel damping of single-phase PWM voltage source converter," *IEEE Transactions on Control Systems Technology*, vol. 22, no. 4, pp. 1310–1322, 2014.
- [4] O. Kukrer, H. Komurcugil, and A. Doganalp, "A three-level hysteresis function approach to the sliding-mode control of single-phase ups inverters," *IEEE Transactions on Industrial Electronics*, vol. 56, no. 9, pp. 3477–3486, Sept 2009.
- [5] M. B. Ketzer and C. B. Jacobina, "Nonlinear control for single-phase universal active filters," in *IECON 2014 - 40th Annual Conference of the IEEE Industrial Electronics Society*, Oct 2014, pp. 202–208.
- [6] D. Karagiannis, E. Mendes, A. Astolfi, and R. Ortega, "An experimental comparison of several pwm controllers for a single-phase ac-dc converter," *IEEE Transactions on Control Systems Technology*, vol. 11, no. 6, pp. 940–947, Nov 2003.
- [7] Y. Boussairi, A. Abouloifa, A. Hamdoun, and C. Aouadi, "Backstepping controller design for a single phase dc/ac converter applied to grid-connected wind energy," in *2015 3rd International Renewable and Sustainable Energy Conference (IRSEC)*, Dec 2015, pp. 1–5.

- [8] M. Pahlevani, S. Eren, A. Bakhshai, and P. Jain, "A voltage control technique for grid-connected single-phase ac/dc converters with g2v/v2g capability," in *2015 IEEE Energy Conversion Congress and Exposition (ECCE)*, Sept 2015, pp. 5400–5405.
- [9] S. Wang, J. Su, X. Yang, Y. Du, Y. Tu, and H. Xu, "A review on the small signal stability of microgrid," *2016 IEEE 8th International Power Electronics and Motion Control Conference, IPEMC-ECCE Asia 2016*, no. 2, pp. 1793–1798, 2016.
- [10] M. Sanatkar-Chayjani and M. Monfared, "Simple digital current control strategy for single-phase grid-connected converters," *IET Power Electronics*, vol. 8, no. 2, pp. 245–254, 2015.
- [11] O. Stihl and B.-T. Ooi, "A single-phase controlled-current pwm rectifier," *IEEE Transactions on Power Electronics*, vol. 3, no. 4, pp. 453–459, Oct 1988.
- [12] G. Rakesh and N. M. Pindoriya, "Simulation and experimental study of single phase pwm ac/dc converter for microgrid application," in *2016 IEEE 1st International Conference on Power Electronics, Intelligent Control and Energy Systems (ICPEICES)*, July 2016, pp. 1–6.
- [13] W. Song, Z. Deng, S. Wang, and X. Feng, "A simple model predictive power control strategy for single-phase pwm converters with modulation function optimization," *IEEE Transactions on Power Electronics*, vol. 31, no. 7, pp. 5279–5289, July 2016.
- [14] P. Acuna, R. P. Aguilera, A. M. Y. M. Ghias, M. Rivera, C. R. Baier, and V. G. Agelidis, "Cascade-free model predictive control for single-phase grid-connected power converters," *IEEE Transactions on Industrial Electronics*, vol. 64, no. 1, pp. 285–294, Jan 2017.
- [15] M. Monfared, M. Sanatkar, and S. Golestan, "Direct active and reactive power control of single-phase grid-tie converters," *IET Power Electronics*, vol. 5, no. 8, pp. 1544–1550, September 2012.
- [16] F. Evran, "Plug-in repetitive control of single-phase grid-connected inverter for ac module applications," *IET Power Electronics*, vol. 10, no. 1, pp. 47–58, 2017.
- [17] A. Kumar, A. H. Bhat, and S. P. Singh, "Performance evaluation of fuzzy logic controlled voltage source inverter based unified power quality conditioner for mitigation of voltage and current harmonics," in *2016 International Conference on Advances in Computing, Communications and Informatics (ICACCI)*, Sept 2016, pp. 1799–1804.

- [18] A. Abrishamifar, A. Ahmad, and M. Mohamadian, "Fixed switching frequency sliding mode control for single-phase unipolar inverters," *IEEE Transactions on Power Electronics*, vol. 27, no. 5, pp. 2507–2514, May 2012.
- [19] M. Monfared, S. Golestan, and J. M. Guerrero, "Analysis, design, and experimental verification of a synchronous reference frame voltage control for single-phase inverters," *IEEE Transactions on Industrial Electronics*, vol. 61, no. 1, pp. 258–269, 2014.
- [20] B. Bahrani, A. Rufer, S. Kenzelmann, and L. A. C. Lopes, "Vector control of single-phase voltage-source converters based on fictive-axis emulation," *IEEE Transactions on Industry Applications*, vol. 47, no. 2, pp. 831–840, 2011.
- [21] S. Dasgupta and S. Sahoo, "Single-Phase Inverter Control Techniques for Interfacing Renewable Energy Sources With Microgrid Part I : Parallel-Connected Inverter Topology With Active and Reactive Power Flow," *Power Electronics, IEEE*, vol. 26, no. 3, pp. 717–731, 2011. [Online]. Available: <http://ieeexplore.ieee.org/xpls/abs{ }all.jsp?arnumber=5657265>
- [22] S. Gerngross and C. P. Dick, "Turnkey solution for single-phase grid-connected dc/ac converter controls," in *PCIM Europe 2014; International Exhibition and Conference for Power Electronics, Intelligent Motion, Renewable Energy and Energy Management*, May 2014, pp. 1–8.
- [23] S. Gautam and R. Gupta, "Unified time-domain formulation of switching frequency for hysteresis current controlled ac/dc and dc/ac grid connected converters," *IET Power Electronics*, vol. 6, no. 4, pp. 683–692, April 2013.
- [24] N. Jaalam, N. Rahim, A. Bakar, C. Tan, and A. M. Haidar, "A comprehensive review of synchronization methods for grid-connected converters of renewable energy source," *Renewable and Sustainable Energy Reviews*, vol. 59, pp. 1471 – 1481, 2016. [Online]. Available: <http://www.sciencedirect.com/science/article/pii/S1364032116000964>
- [25] G. C. Konstantopoulos and Q. C. Zhong, "Current-limiting non-linear controller for single-phase ac/dc pwm power converters," in *2015 American Control Conference (ACC)*, July 2015, pp. 1029–1034.
- [26] Y.-N. Tong, C.-L. Li, and F. Zhou, "Synchronization control of single-phase full bridge photovoltaic grid-connected inverter," *Optik - International Journal for Light and Electron Optics*, vol. 127, no. 4, pp. 1724 – 1728, 2016. [Online]. Available: <http://www.sciencedirect.com/science/article/pii/S0030402615016800>

- [27] N. Mohan, T. Undeland, and W. Robbins, *Power Electronics: Converters, Applications and Design*, ser. And Its Applications. Wiley, 1989. [Online]. Available: <https://books.google.co.in/books?id=CiNXAAAAIAAJ>
- [28] C. Cho, J. H. Jeon, J. Y. Kim, S. Kwon, K. Park, and S. Kim, “Active synchronizing control of a microgrid,” *IEEE Transactions on Power Electronics*, vol. 26, no. 12, pp. 3707–3719, 2011.
- [29] J. Machowski, J. Bialek, and J. Bumby, *Power System Dynamics: Stability and Control*, . John Wiley & Sons, Ed. Wiley, 2011.
- [30] Y. Han, M. Luo, X. Zhao, J. M. Guerrero, and L. Xu, “Comparative performance evaluation of orthogonal-signal-generators-based single-phase pll algorithms – a survey,” *IEEE Transactions on Power Electronics*, vol. 31, no. 5, pp. 3932–3944, May 2016.
- [31] M. Ciobotaru, R. Teodorescu, and F. Blaabjerg, “A new single-phase pll structure based on second order generalized integrator,” in *2006 37th IEEE Power Electronics Specialists Conference*, June 2006, pp. 1–6.
- [32] P. Rodriguez, A. Luna, R. S. Muñoz-Aguilar, I. Etxeberria-Otadui, R. Teodorescu, and F. Blaabjerg, “A stationary reference frame grid synchronization system for three-phase grid-connected power converters under adverse grid conditions,” *IEEE Transactions on Power Electronics*, vol. 27, no. 1, pp. 99–112, Jan 2012.
- [33] P. Rodriguez, A. Luna, I. Candela, R. Teodorescu, and F. Blaabjerg, “Grid synchronization of power converters using multiple second order generalized integrators,” in *2008 34th Annual Conference of IEEE Industrial Electronics*, Nov 2008, pp. 755–760.
- [34] J. A. Suul, K. Ljokelsoy, and T. Undeland, “Design, tuning and testing of a flexible pll for grid synchronization of three-phase power converters,” in *2009 13th European Conference on Power Electronics and Applications*, Sept 2009, pp. 1–10.
- [35] R. T. M. L. P. Rodriguez, *Grid Converters for Photovoltaic and Wind Power Systems*. Wiley-IEEE Press, 2011.
- [36] B. Bahrani, A. Rufer, S. Kenzelmann, and L. A. C. Lopes, “Vector control of single-phase voltage-source converters based on fictive-axis emulation,” *IEEE Transactions on Industry Applications*, vol. 47, no. 2, pp. 831–840, March 2011.

- [37] M. Vasiladiotis and A. Rufer, “Fictive axis emulator-based state feedback vector current control for single-phase voltage source converters,” in *IECON 2013 - 39th Annual Conference of the IEEE Industrial Electronics Society*, Nov 2013, pp. 773–778.
- [38] S. Somkun and V. Chunkag, “Simple and fast synchronous reference frame current control for single-phase grid-connected voltage source converters,” in *IECON 2015 - 41st Annual Conference of the IEEE Industrial Electronics Society*, Nov 2015, pp. 002 276–002 281.
- [39] M. Ebrahimi, S. A. Khajehoddin, and M. Karimi-Ghartemani, “Fast and robust single-phase dq current controller for smart inverter applications,” *IEEE Transactions on Power Electronics*, vol. 31, no. 5, pp. 3968–3976, May 2016.
- [40] H. Khalil, *Nonlinear Systems*. Prentice Hall, 2000. [Online]. Available: https://books.google.no/books?id=v_BjPQAACAAJ